Chemical Engineering Journal 500 (2024) 157321

Contents lists available at ScienceDirect

Chemical Engineering Journal

journal homepage: www.elsevier.com/locate/cej

Review

Chemical looping based Low-pressure ammonia synthesis

Hangzuo Guo [a], Alexander R.P. Harrison [a,d], Mingchen Gao [a], Xusheng Zhang [b], Qicheng Chen [c], Zhanfeng Cui [a], Binjian Nie [a,*]

[a] Department of Engineering Science, University of Oxford, Oxford OX1 3PJ, United Kingdom
[b] Birmingham Centre for Energy Storage, School of Chemical Engineering, University of Birmingham, Birmingham B15 2TT, United Kingdom
[c] School of Energy and Power Engineering, Northeast Electric Power University, Jilin 132012, China
[d] Department of Chemical Engineering and Biotechnology, University of Cambridge, Philippa Fawcett Drive, CB3 0AS Cambridge, United Kingdom

ARTICLE INFO

Keywords:
Ammonia synthesis
Chemical looping
Nitrogen carrier
Imide-hydride
Metal nitride

ABSTRACT

Ammonia (NH_3) is a promising alternative to fossil fuels due to its ability to store and release hydrogen without carbon emissions, with high energy density. The traditional Haber-Bosch (H-B) process for ammonia synthesis is energy-intensive, requiring extreme pressure conditions (10–20 MPa). Chemical Looping-based Ammonia Synthesis (CLAS) offers a sustainable alternative, *via* a cyclic process where hydrogen gas reacts with a nitrogen containing solid (termed a 'nitrogen carrier') at near ambient pressure to form ammonia. The nitrogen carrier is regenerated in N_2 gas in a separate step. However, practical implementation of CLAS faces challenges, primarily in the development of effective nitrogen carriers. This review analyses nitrogen carrier materials for the CLAS process, focusing on material screening and fabrication techniques, as well as strategies to reduce energy consumption and increase ammonia production at reactor and system level. The latest advancements in transition metal nitrides and alkali/alkaline earth metal imides are highlighted, as well as external field-assisted technologies to apply the CLAS process at industrial scale.

1. Introduction

Energy has always been a pivotal factor to drive the progress of civilization and economic development. Nevertheless, the economic framework reliant on fossil fuels presents numerous obstacles, such as substantial carbon dioxide emissions, alongside air pollution from harmful combustion products such as soot [1]. Hence, novel technologies have been investigated to implement non-carbonaceous fuels for energy generation and transportation, such as hydrogen [2]. Ammonia holds significant advantages as a medium for storing energy in the form of hydrogen. The formation enthalpy of ammonia ($\Delta H^0_{298\ K} = -46$ kJ/mol) is intermediate between the high stability of water (H_2O, $\Delta H^0_{298\ K}$ = -286 kJ/mol) and the low stability of hydrogen gas (H_2, $\Delta H^0_{298\ K} =$ 0 kJ/mol) [3,4]. The moderate stability allows ammonia to store hydrogen in the NH_3 molecule, which can then be decomposed to produce hydrogen gas when energy is needed. When ammonia is decomposed catalytically, nitrogen is the only other product, meaning ammonia can be used to reversibly store chemical energy without emitting carbon dioxide [5]. Ammonia has a relatively high gravimetric hydrogen density (17.7 wt%) and energy density (3 kWh/kg), making it an ideal energy medium and hydrogen carrier [6,7]. The dominant Haber-Bosch (H-B) process for producing ammonia involves two main stages: feed gas preparation and ammonia production. The core of the ammonia production process is the reaction of purified H_2 and N_2 over an iron-based catalyst at high temperature and pressure, at 500-600℃ and 10–20 MPa respectively, and the per-pass conversion efficiency is relatively low (only 10–15 %), requiring a further separation process [8,9]. Currently, the Haber-Bosch process consumes nearly 2 % of the world's electricity production and emits over 400 million tons of CO_2 annually, accounting for 1.6 % of global carbon emissions [9,10]. Alternative catalysts with higher activities than Fe, such as Ru [11], have been applied for more efficient Haber-Bosch synthesis. However, it still requires high temperatures and pressures (300–500 °C, >100 bar), making further reductions in energy consumption challenging [9,12]. With an increasing understanding of ammonia synthesis mechanisms [13–15], researchers have been exploring new methods for green

Abbreviations: AMH, Alkali metal/Alkaline earth metal hydride; AMN, Alkali metal/Alkaline earth metal nitride; AMNH, Alkali metal/Alkaline earth metal imide; CLAS, Chemical looping ammonia synthesis; H-B, Haber-Bosch; MN, Metal nitride; PTMN, Post-transition metal nitride; TMN, Transition metal nitride.

* Corresponding author.
E-mail address: binjian.nie@eng.ox.ac.uk (B. Nie).

https://doi.org/10.1016/j.cej.2024.157321
Received 12 August 2024; Received in revised form 8 October 2024; Accepted 31 October 2024
Available online 1 November 2024
1385-8947/© 2024 The Author(s). Published by Elsevier B.V. This is an open access article under the CC BY license (http://creativecommons.org/licenses/by/4.0/).

Table 1
Comparison of different technologies for NH_3 production [25,31].

Parameters	Thermocatalytic Process (Haber-Bosch)	Electrochemical Process (High Temperature)	Electrochemical Process (Low Temperature)	Photocatalytic Process	Plasma Process	Chemical Looping Process
N_2 Source	N_2 (air separation)	N_2 (air separation)	N_2 (air separation)	N_2 (air separation)	N_2 (air separation)	N_2 (air separation)
H_2 Source	H_2	H_2/H_2O	H_2O	H_2O	H_2 (plasma discharge)	H_2/H_2O
Pressure (MPa)	15–25	Ambient	Ambient	Ambient	Ambient	Ambient
Reaction Temp. (℃)	400–450	400–700 (solid state)	Ambient	Ambient	25–200	500–1300
NH_3 Yield/ Conversion Rate	15 % per pass	78 % H_2 utilization (solid state, from H_2)	Low (<100 μg/cm^2·h)	N/A	~85 %	~88 %
Energy Efficiency	62–65 %	88.5 %	~14 %	N/A	~90 %	~70 %
Byproducts	CO_2	None	None	None	None	None
N_2 Activation Mode	Dissociative	Associative	Associative	Associative	Dissociative	Dissociative
Rate-Determining Step	N_2 dissociation to N atoms	N_2 hydrogenation to N_2H^*	N_2 hydrogenation to N_2H^*	N_2 hydrogenation to N_2H^*	N_2 dissociation to N atoms	N_2 dissociation to N atoms
Development Stage	Industrial	Research stage	Research stage	Research stage	Research stage	Research stage
Energy Input	Heat	Electricity	Electricity	Light	Electricity (plasma)	Heat/ (Electricity or Light)

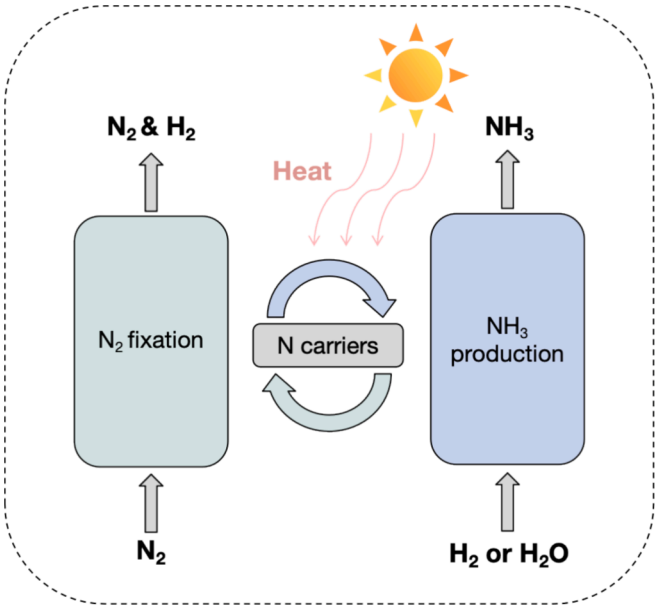


Fig. 1. Schematic of chemical looping ammonia synthesis.

ammonia synthesis. They include electrocatalysis [15–19], photocatalysis [20–22], plasma-assisted synthesis [23–25] and chemical looping [26–28], which has shown potential for green ammonia production [29]. Despite significant advances in photocatalysis, electrocatalysis and plasma-assisted synthesis for green ammonia production, key issues of these technologies, such as ammonia synthesis rates, energy conversion efficiency, and catalyst stability, remain unresolved, limiting their large-scale application.

Chemical Looping based Ammonia Synthesis (CLAS, also referred to as CLAP, CLAG, or CL-NH_3 in literature) divides the traditional single-step process into multiple sub-reactions, allowing optimization of each reaction step. The multi-step approach mitigates competitive adsorption of the H_2 and N_2 on the catalysts' surface, and certain inorganic nitrogen compounds used in the chemical looping process are sufficiently reactive to allow operation at near-ambient pressure [30]. Existing CLAS research focuses on reaction pathways and nitrogen carriers, but systematic review on nitrogen carrier design is still lacking. This paper presents a comprehensive review of the selection, preparation and modification of materials utilized in CLAS, as well as recent approaches in reactor design and pathways for future improvements. A comparison of CLAS with the Haber-Bosch process and other technologies for NH_3 production is given in Table 1.

2. Chemical looping for ammonia synthesis

Chemical looping-based ammonia synthesis involves multiple steps. First, gaseous N_2 is fixed with a nitrogen catalyst (*e.g.,* a metal hydride or N-deficient nitride) to form a nitrogen-containing compound, termed as a nitrogen carrier [32]. Then, the nitrogen carrier reacts with hydrogen or water to form ammonia through hydrogenation or hydrolysis, meanwhile, the nitrogen catalyst is regenerated, and the chemical loop is completed (see Fig. 1) [29,33]. The CLAS avoids competitive adsorption of hydrogen or water with nitrogen on the active sites of the catalyst, whereas in traditional H-B synthesis, catalyst poisoning can occur because of excessively strong adsorption of N_2 or H_2 [3,34].

The performance and operating conditions of the CLAS heavily depend on the nitrogen carrier to be used, as well as the thermodynamic and kinetic properties of each step. According to different types of nitrogen carriers, CLAS can be divided into two main pathways: metal nitride-based (MN-CLAS) and alkali/alkaline earth metal imide-based (AMNH-CLAS) pathways [35]. Alternatively, CLAS can be classified into two pathways by different hydrogen sources: H_2O-CLAS, which uses water as the hydrogen source, and H_2-CLAS, which uses hydrogen gas directly (Fig. 2).

2.1. Metal nitride as N carriers

Metal nitrides (MN) are relatively easy to prepare from the reduction of the metal oxides or the nitridation of metals [36], making them widely studied as nitrogen carriers. Both H_2O and H_2 can react with MN to enable CLAS, as shown in Fig. 2a. and Fig. 2b., respectively. The thermodynamics of ammonia production from hydrogen sources and the regeneration performance of MN are critical for MN-CLAS [37]. In metal nitrides, nitrogen exists as nitride ions (N^{3-}), and their chemical properties vary according to the changes in the valence electron configuration of the metal. MN can be categorized into post-transition metal nitrides (PTMN), transition metal nitrides (TMN), and alkali and alkaline earth metal nitrides (AMN) [28].

2.1.1. Post-transition metal nitrides

Post-transition metal nitrides (PTMN), such as aluminum nitride (v), were among the first materials used as nitrogen carriers in CLAS [38–40]. Given that PTMN materials often exhibit high thermal and chemical stability, relatively high temperatures are required to operate the chemical loop (>1000℃). In a H_2O-MN-CLAS process, the PTMN typically reacts with steam to synthesize ammonia, bypassing the need

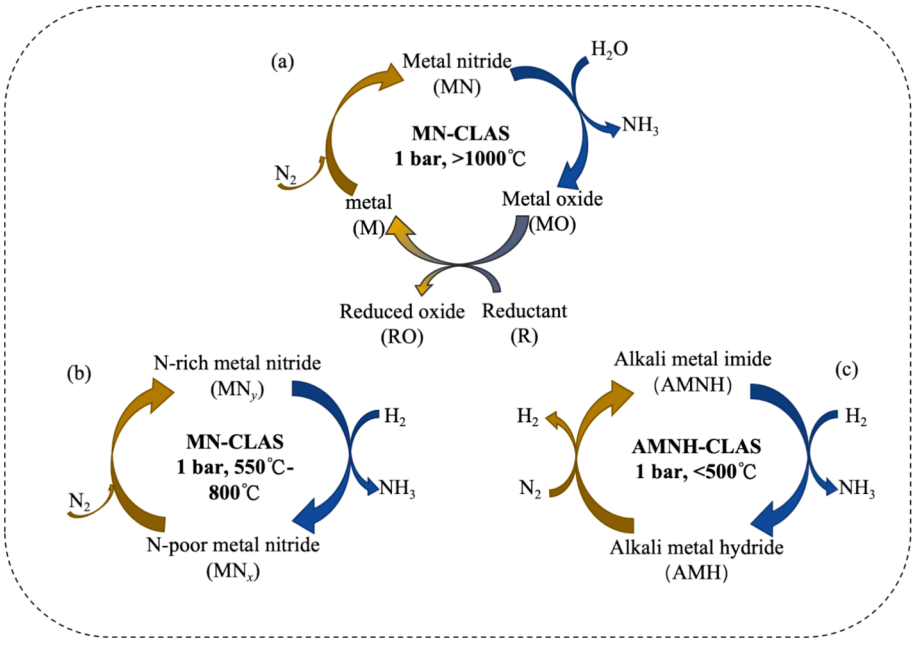


Fig. 2. Schematics of CLAS mediated by a metal nitride using (a) H_2O and (b) H_2 as hydrogen source, and (c) CLAS mediated by an alkali metal.

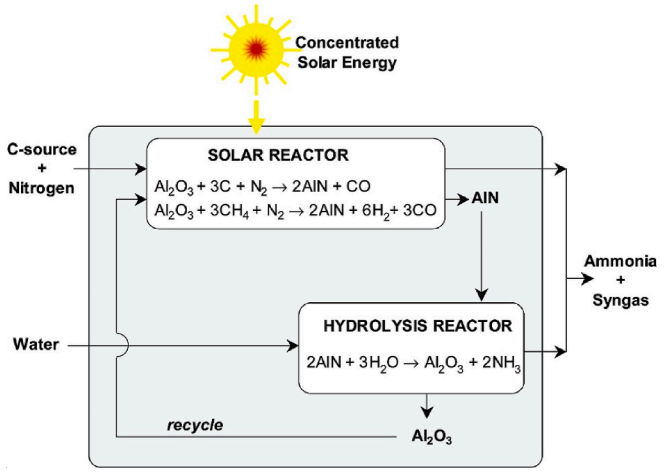


Fig. 3. Scheme of the H_2O-CLAS process via solar energy mediated Al_2O_3/AlN [39]. Copyright 2007, American Chemical Society.

to produce green hydrogen gas by electrolysis [41]. In 2007, Steinfeld et al. [38–40] proposed a solar-driven, two-step chemical looping process for ammonia synthesis, as shown in Fig. 3. Their process involved the reduction of Al_2O_3 with methane or carbon to form AlN and CO; subsequently, AlN reacted with steam to produce ammonia and Al_2O_3 was regenerated. The reactions are as follows (Eqs. 1–3) with thermodynamic properties reported in Table 2.

N_2 Fixation & Reduction:

$$Al_2O_3 + 3C + N_2 \rightarrow 2AlN + 3CO \quad (1)$$

$$Al_2O_3 + 3CH_4 + N_2 \rightarrow 2AlN + 6H_2 + 3CO \quad (2)$$

NH_3 Production:

$$2AlN + 3H_2O \rightarrow Al_2O_3 + 2NH_3 \quad (3)$$

However, the nitrogen fixation reaction is highly endothermic, requiring 1500-2000℃ for reducing AlN/Al_2O_3 to AlN, causing significant energy consumption and high equipment requirements [42,43]. Additionally,

Table 2
Thermodynamic properties of reactions of MN nitrogen carriers. (Values are calculated using FactSage 8.3 software, using the FactPS thermodynamic database[63]).

Reactions	ΔH° 298 K (kJ/mol)	ΔS° 298 K (J/mol·K)	ΔG° 298 K (kJ/mol)
$Al_2O_3 + 3C + N_2 \rightarrow 2AlN + 3CO$	708.1	353.2	920.9
$Al_2O_3 + 3CH_4 + N_2 \rightarrow 2AlN + 6H_2 + 3CO$	932.8	615.5	749.3
$2AlN + 3H_2O \rightarrow Al_2O_3 + 2NH_3$	−406.0	−170.3	−355.3
$2Cr + 1/2N_2 \rightarrow Cr2N$	−125.5	−78.0	−102.3
$Cr_2N + 3H_2O \rightarrow Cr_2O_3 + NH_3 + 3/2H_2$	−322.0	−157.8	−275.0
$Cr_2O_3 + 3H_2 \rightarrow 2Cr + 3H_2O$	401.6	136.8	360.9
$Cr_2O_3 + 3CO \rightarrow 2Cr + 3CO_2$	278.1	11.1	274.8
$5Mn + N_2 \rightarrow Mn_5N_2$	−204.2	−164.1	−155.3
$1/2Mn_5N_2 + 5/2H2O \rightarrow 5/2MnO + NH_3 + H_2$	−301.5	−92.7	−273.9
$MnO + CH_4 \rightarrow Mn + CO + 2H_2$	349.3	244.7	276.3
$2Mo + 1/2N_2 \rightarrow Mo_2N$	−81.6	−89.8	−54.8
$Mo_2N + 4H_2O \rightarrow 2MoO_2 + NH_3 + 5/2H_2$	−172.7	−206.1	−111.3
$MoO_2 + 2CO \rightarrow Mo + 2CO_2$	21.9	14.7	17.5
$MoO_2 + 2H_2 \rightarrow Mo + 2\,H_2O$	104.2	98.5	74.8

prolonged operation at high temperatures can decrease the solids' surface area and pore volume which limited the materials' cycling life [44,45]. Furthermore, while AlN hydrolysis is thermodynamically feasible, the reaction kinetics are slow. However, an advantage of Al_2O_3-based materials is that the α-Al_2O_3 phase has been shown from experimental and computational studies to inhibit the decomposition of NH_3 to N_2 and H_2 [46], increasing the maximum achievable yield of ammonia during hydrolysis over partially converted AlN/Al_2O_3. Doping AlN/Al_2O_3 nitrogen carriers with ZrO_2 was also found to mitigate ammonia decomposition [47,48], by formation of chemisorbed NH_3 species on at Lewis acidic sites [49], which subsequently desorb without decomposing.

Gallium nitride (GaN) has also been considered theoretically for a three-step H_2O-CLAS process [50], using non-thermal plasma to reduce

Ga_2O_3 to liquid metal Ga, which then reacts with N_2 gas to form GaN. The proposed system showed highly favorable thermodynamics for NH_3 formation and N-fixation, however, the feasibility of the process has yet to be demonstrated experimentally in a practical unit. The nitrides of the other post-transition metals (In, Sn, Tl, Pb, Bi, Po) have not been investigated for CLAS processes.

2.1.2. Transition metal nitrides

Transition metal nitrides (TMN) have been applied in various applications in recent years for their good electrical conductivity, chemical stability, and catalytic properties [36,51]. For the CLAS process, TMN materials can produce ammonia by hydrolysis through reaction with H_2O (*e.g.*, Cr_2N, Mn_5N_2, Mo_2N [52,53]) or by direct reaction with H_2 (*e.*

Table 3
The operating conditions and NH_3 production rate of various N carriers.

System	N carriers	N carrier pairs	Condition			NH_3 production rate ($\mu mol\ g^{-1}h^{-1}$)	Ref.
			Regeneration	Nitridation	Denitridation		
Haber–Bosch process	Fe-based catalysts	Al_2O_3-$Fe_{1-x}O$	430℃ & 30 bar			11,900	[73]
		Al_2O_3-Fe_3O_4	430℃ & 30 bar			9,200	[73]
		K-Al_2O_3-FeOOH	500℃ & 90 bar			32,850	[74]
	Ru-based catalysts	BaO-CaH_2-Ru	340℃ & 1 bar			10,500	[75]
		MgO-Cs-Ru	400℃ & 26 bar			4,200	[76]
H_2O-CLAS	Metal Nitride	AlN/Al_2O_3	1500 ~ 2000℃		1200℃	–	[77]
		ZrO_2-AlN/Al_2O_3	1000℃		1000℃	850	[47]
		NaOH-Mn_5N_2/MnO	1150℃		500℃	–	[62]
		Cr/Cr_2N/Cr_2O_3	500 ~ 1000℃	1200 ~ 1500℃	1000℃	124	[52,78]
		Mo/Mo_2N/MoO_2	750 ~ 1200℃	750 ~ 850℃	500℃	1,200.6	[53]
		Mn/Mn_5N_2/MnO	1000 ~ 1230℃	1000 ~ 1150℃	500℃	–	[53]
		Mn/Mn_4N_2/MnO	1400℃	700℃	500℃	635.7	[52]
		Mg/Mg_3N_2/MgO	1800℃	1200℃	500℃	–	[52]
		Ca/Ca_3N_2-Ca_2N/CaO	2000℃	1200℃	200℃	–	[52]
		Zn/Zn_3N_2/ZnO	1000℃	1200℃	500℃	–	[52]
		e-Li/Li_3N/LiOH	450℃ & 3 V	22 ~ 100℃	120℃	–	[79]
		l-TiN-Mg/Mg_3N_2/MgO	550℃ & 30 W/cm^2	550℃ & 30 W/cm^2	550℃ & 30 W/cm^2	1.67	[80]
H_2-CLAS		$MnN_{x-\delta}$/MnN_x	800℃		400℃	51.2	[57]
		Li-$MnN_{x-\delta}$/MnN_x	800℃		500℃	414.4	[57]
		Mo/Mo_2N	600℃		450℃	4,576	[58]
		Co_6Mo_6N/Co_3Mo_3N	700℃		500℃	98	[59]
		Ni_2Mo_3N/$Ni_2Mo_3N_{1-x}$	700℃		400℃	11	[59]
		$Mn_6N_{2.58}$/Mn_4N	700℃		550℃	61.5	[54]
		SrH_2/Sr_2N	700℃		550℃	87.6	[54]
		Ca_2NH/Ca_3N_2	700℃		550℃	120.9	[54,81]
		Fe/Fe_3N	500℃		400℃	50	[55]
		Re/Re_3N	700℃		350℃	130	[55]
		Cu/Cu_3N	–		250℃	665	[56]
		Ni/NiN_3	480℃		250℃	757.5	[56]
		Zn/Zn_3N_2	–		400℃	852	[56]
		Ta/Ta_3N_5	700℃		400℃	80	[56]
		Re-Ta/$Ta_{2.5}Re_{0.5}Ny$	–		500℃	23.1	[82]
		Fe-Ta/$Ta_{2.5}Fe_{0.5}Ny$	–		500℃	25.1	[82]
		Co-Ta/$Ta_{2.5}Co_{0.5}Ny$	–		500℃	250.8	[82]
		Co-Zn/Co_3ZnN	–		500℃	581.8	[83]
		Ni-Zn/Ni_3ZnN	–		500℃	576.8	[83]
		Co-In/Co_3InN	–		500℃	253.8	[83]
		Ni-In/Ni_3InN	–		500℃	467.3	[83]
		MWP-FeN_x/FeN_y	250℃		450℃	6,313.5	[84]
		Sn-Li/LiN_3/LiH	500℃	500℃	240℃	120	[85]
	Metal imides	Li_2NH/LiH	350℃		350℃	100	[86]
		Pd-Li_2NH/LiH	300℃		300℃	700	[86]
		Zn-Li_2NH/LiH	350℃		350℃	956	[87]
		Ni-Li_2NH/LiH	300℃		300℃	1,533	[30]
		BaNH/BaH_2	350℃		350℃	198	[30]
		Fe-BaNH/BaH_2	300℃		300℃	1,703	[30]
		Co-BaNH/BaH_2	300℃		300℃	1,866	[30]
		Ni-BaNH/BaH_2	300℃		300℃	3,125	[30]
		Ni-MgO-BaNH/BaH_2	250℃		250℃	1,530	[30]
		Ni-Al_2O_3-BaNH/BaH_2	250℃		250℃	2,770	[30]
		molten salt-Li_2NH/LiH	400℃		400℃	914	[88]
		e-molten salt-Li_2NH/LiH	400℃ & 2 V		400℃ & 2 V	2,058	[88]
		p-$NaNH_2$/NaH	300℃ & 12 kV		25 ~ 250℃ & 12 kV	550	[89]
		p-MgO-$NaNH_2$/NaH	300℃ & 12 kV		25 ~ 250℃ & 12 kV	2,080	[89]
		p-molten salt-KNH_2/KH	–		25 ~ 250℃ & 12 kV	1,100	[89]
		p-MgO-KNH_2/KH	–		25 ~ 250℃ & 12 kV	842	[89]
		Cr-Li_2NH/LiH	300℃ & 10 bar		300℃ & 10 bar	3,600	[90]
		Mn-Li_2NH/LiH	300℃ & 10 bar		300℃ & 10 bar	3,100	[90,91]
		Fe-Li_2NH/LiH	300℃ & 10 bar		300℃ & 10 bar	4,450	[90,91]
		Co-Li_2NH/LiH	300℃ & 10 bar		300℃ & 10 bar	4,200	[90,91]
	Metal imides-nitrides	Mn_2N/Li_2NH-Mn_4N/LiH	200℃		300℃	1,576	[92]
		Mn_2N/BaNH-Mn_4N/BaH_2	225℃		300℃	3,142	[92]

e: electro-driven; l: light-driven; p: plasma-driven; MWP:Microwave-plasma-assisted.

g., Ti_3N_2, Co_3Mo_3N, Mo_2N, Mn_3N_2 and Ni_3N [54–59]). In 2011, Pfromm et al. [60] proposed a three-step CLAS method based on the $Cr/Cr_2N/Cr_2O_3$ cycle. Initially, Cr is nitrided to form Cr_2N which then reacts with H_2O to produce NH_3. Finally, the Cr_2O_3 is reduced by CO or H_2 to regenerate Cr. The reactions are as follows (Eqs. 4–7), with thermodynamic properties reported in Table 2:

N_2 Fixation:

$$2\,Cr + 1/2\,N_2 \rightarrow Cr_2N \tag{4}$$

NH_3 Production:

$$Cr_2N + 3H_2O \rightarrow Cr_2O_3 + NH_3 + 3/2H_2 \tag{5}$$

Reduction:

$$Cr_2O_3 + 3H_2 \rightarrow 2Cr + 3H_2O \tag{6}$$

$$Cr_2O_3 + 3CO \rightarrow 2Cr + 3CO_2 \tag{7}$$

Compared to the AlN system, the Cr_2N system requires two steps for Cr_2O_3 reduction, followed by nitrogen fixation. While using a gas-phase reductant can lower the temperature required for Cr_2O_3 reduction compared to that of solid-phase reductant, it still necessitates high temperatures (1200-1600℃). Besides, the nitrogen fixation and ammonia production steps still require high temperatures (500-1000℃) due to slow intrinsic reaction kinetics [60,61]. Molybdenum- and manganese-based TMN nitrogen carriers (Mo_2N and Mn_5N_2) are also considered promising for CLAS [62]. Like the $Cr/Cr_2N/Cr_2O_3$ cycle, Mo and Mn metals react with nitrogen to form Mo_2N and Mn_5N_2, which will then be hydrolyzed to form MoO_2 and MnO. The oxides are further regenerated to metals using gas-phase reductants (*e.g.,* CH_4). Compared to the Cr_2N system, Mo_2N and Mn_5N_2 show superior thermodynamic properties, allowing reduction at 1150℃ and nitrogen fixation at 800℃, as well as hydrolysis at 500℃ and higher ammonia production rates. The reactions are given below (Eqs. 8–13), with thermodynamic properties reported in Table 2:

N_2 Fixation:

$$5\,Mn + N_2 \rightarrow Mn_5N_2 \tag{8}$$

NH_3 Production:

$$1/2Mn_5N_2 + 5/2H_2O \rightarrow 5/2MnO + NH_3 + H_2 \tag{9}$$

Reduction:

$$5/2MnO + 5/2CH_4 \rightarrow 5/2Mn + 5/2CO + 5H_2 \tag{10}$$

N_2 Fixation:

$$2Mo + 1/2N_2 = Mo_2N \tag{11}$$

NH_3 Production:

$$Mo_2N + 4H_2O = 2MoO_2 + NH_3 + 5/2H_2 \tag{12}$$

Reduction:

$$MoO_2 + 2CO = Mo + 2CO_2 \tag{13a}$$

$$MoO_2 + 2H_2 = Mo + 2H_2O \tag{13b}$$

In hydrolysis-based chemical loops, the resulting oxides are highly stable and require high temperatures for reduction, leading to lower overall energy efficiency, and limiting industrial applicability (*e.g.,* from solar concentration as implemented in [38–40]). An alternative process is H_2-CLAS, as shown in Eqs. 14–15, which involves nitrogen fixation by reacting a nitrogen deficient metal nitride with gaseous nitrogen to form a nitrogen-rich carrier, which is then reacted with hydrogen to produce ammonia. This simpler pathway is suitable for distributed ammonia production [64], allows relatively low-temperature processes (typically below 800℃), and facilitates green ammonia synthesis under mild conditions [27,65].

N_2 Fixation & Reduction:

$$TM_aN_{b-x} + x/2N_2 \rightarrow TM_aN_b \tag{14}$$

NH_3 Production:

$$TM_aN_b + 3x/2H_2 \rightarrow TM_aN_{b-x} + xNH_3 \tag{15}$$

Original TMN, such as TiN [26], has excessively high nitrogen vacancy formation energies, and the accumulation of N atoms on the surface leads to slow hydrogenation reaction kinetics. Suitable stability of the TMN is a key factor influencing their nitrogen fixation and ammonia production performance [66–68]. The kinetics of nitrogen carriers are like traditional catalysts: Ideal catalysts for ammonia synthesis should have moderate nitrogen adsorption strength; strong adsorption (*e.g.*, Re, Mo) hinders ammonia desorption, while weak adsorption (*e.g.*, Pt, Ni) impedes nitrogen activation. The Co-Mo nitride system represents a significant advancement over traditional Fe and Ru catalysts [33]. Hargreaves et al. [69–71] discovered that the Co_3Mo_3N catalyst exhibits reversible lattice nitrogen cycling when alternately exposed to H_2 and N_2. During H_2 exposure, a portion of the lattice nitrogen is released as ammonia, forming Co_6Mo_6N. Subsequently, upon exposure to N_2, Co_6Mo_6N is regenerated back to Co_3Mo_3N. Isotope exchange experiments confirmed the activity and reversibility of lattice nitrogen, highlighting Co_3Mo_3N's potential as a nitrogen carrier for CLAS. Further studies extended to Cu_3N, Ni_3N, Zn_3N_2 and Ta_3N_5 [56]. Cu_3N and Ni_3N demonstrated relative instability, with 30 % of lattice nitrogen converting to NH_3 at 250℃. Zn_3N_2 and Ta_3N_5 exhibited lower reactivity, with Ta_3N_5 showing the lowest ammonia production rate but the best renewability. At 700℃, Ta_3N_5 could regenerate nearly 100 % of its nitrogen through ammonia decomposition. Research [55] on Fe_3N, Co_4N, and Re_3N indicated similar ammonia production performance to earlier nitrogen carriers but with poor nitrogen fixation (10–30 wt./mol% lower than 100 *per* chemical looping cycle compared to Ta_3N_5) [48].

Michalsky et al. [54] used electronic structure predictions to advise that Cr_2N and Mn_4N should be thermodynamically favorable for nitridation but unfavorable for hydrogenation, whereas Fe_4N had favorable hydrogenation thermodynamics but unfavorable for nitrogen fixation [72]. Manganese nitrides, such as Mn_4N, with varied valence states and structures, showed suitable thermodynamics for nitrogen fixation and hydrogenation. Hydrogenation of $Mn_6N_{2.58}$ to Mn_4N was experimentally verified at 550℃ but with a low ammonia production rate of 55μmol $g^{-1}h^{-1}$ in the subsequent hydrogenation step. Song et al. [58] developed a Mo_2N/Mo pathway for H_2-MN-CLAS, where metallic Mo reacted with N_2 at 600℃ to form Mo_2N, which was then reacted with H_2 at 450℃ to produce NH_3, both under atmospheric pressure. Compared to the conventional catalytic reaction of H_2 and N_2, this process significantly enhanced nitridation and ammonia synthesis rates over three times, achieving a 4576μmol $g^{-1}h^{-1}$ ammonia synthesis rate at 450℃ without significant degradation during cycling. The operating conditions and NH_3 production rate of the N carriers are summarized in Table 3.

2.1.3. Alkali and alkaline earth metal nitrides (AMN)

Alkali and alkaline earth metals have relatively low ionization energies, electronegativity, and density, making them strong electron donors. They can react with various elements to form diverse complexes [93]. All alkali metals and alkaline earth elements can form nitrides (AMN) [32,67]. TMN, AMN can be hydrolyzed to produce ammonia or react with H_2 to generate ammonia. Common nitrides used in CLAS include Li_3N, Ba_3N_2, Sr_3N_2, Ca_3N_2, Mg_3N_2, and Be_3N_2 [28]. In H_2O-CLAS, AMN (*e.g.,* Li_3N, Mg_3N_2) can react with water at relatively low temperatures to produce ammonia and the corresponding metal oxides or hydroxides, typically achieving fast ammonia production rates [28]. However, regenerating the oxides or hydroxides to form the nitride is

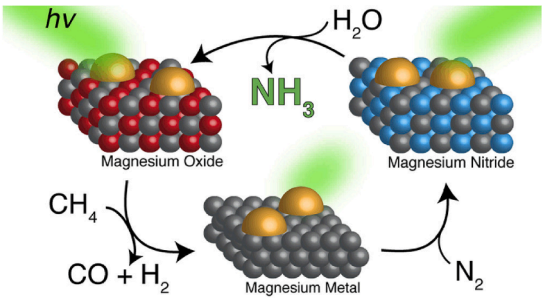


Fig. 4. Schematic diagram of light-driven chemical looping experiments within Mg_3N_2 as nitride[80]. Copyright 2019, American Chemical Society.

thermodynamically challenging and cannot be achieved efficiently through a purely thermal process. Instead, it requires external assistance, such as in electrochemical or photochemical methods. TMN, AMN can be hydrolyzed to produce ammonia or react with H_2 to generate ammonia.

Lithium, compared to other AMNs, has a low standard reduction potential and good lattice structure flexibility [94], allowing it to form strong bonds with nitrogen atoms and dissociate N_2. Consequently, lithium can react with N_2 at room temperature to form stable Li_3N, which can then be hydrolyzed to LiOH and ammonia. However, reducing LiOH to metallic lithium is thermodynamically difficult, and the low melting point of LiOH (471℃) can cause separation issues during regeneration due to melting and, or vaporization. McEnaney et al. [95] proposed an electrochemical method using lithium for chemical looping *via* a three-step process described in Eqs 13–17. In this process, molten LiOH was electrolyzed at 3 V to reduce to Li at 450℃. Then, the Li metal was nitrogenated at 22-100℃ to form Li_3N, which was subsequently hydrolyzed at 22-100℃ to release lattice nitrogen and form ammonia. This process demonstrated high reaction performance with 88.5 % current efficiency for LiOH electrolysis and nearly 100 % conversion in nitrogen fixation and ammonia production stages.

N_2 Fixation:

$$6\,Li + N_2 \rightarrow 2\,Li_3N \tag{16}$$

NH_3 Production:

$$2\,Li_3N + 6\,H_2O \rightarrow 6\,LiOH + 2\,NH_3 \tag{17}$$

LiOH Electrolysis Reduction:

$$6\,LiOH \rightarrow 6\,Li + 3\,H_2O + 3/2\,O_2 \tag{18}$$

$$6\,Li^+ + 6\,e^- \rightarrow 6\,Li \tag{19}$$

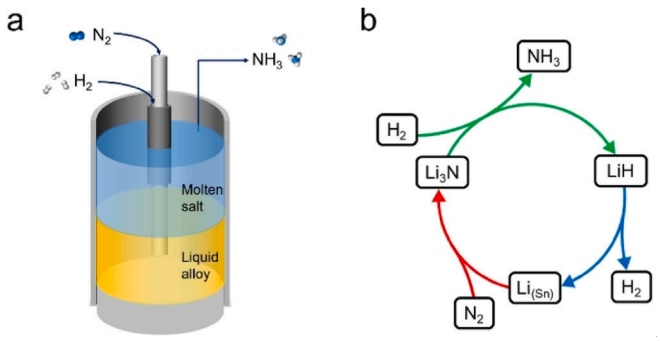


Fig. 5. The combination of liquid Li − Sn alloy and molten eutectic LiCl − KCl salt for NH_3 synthesis (a); Li-based chemical loop for NH_3 synthesis(b)[101]. Copyright 2021 Wiley.

$$6\,OH^- \rightarrow 3\,H_2O + 3/2\,O_2 + 6\,e^- \tag{20}$$

Mg_3N_2 is another AMN nitrogen carrier with the capability to produce ammonia *via* hydrolysis. Magnesium-based materials exhibit favorable thermodynamics for nitrogen fixation and ammonia production. However, regenerating Mg_3N_2 is challenging, as it requires high temperatures (above 1500℃) for carbothermal reduction, which can also lead to the decomposition of the product. Swearer et al. [80] developed a photothermal-driven CLAS pathway using plasma-modified Mg_3N_2 and the cycle, as shown in Fig. 4. In this process, MgO was photothermally reduced to Mg in a CH_4 atmosphere. The Mg then reacted with N_2 to form Mg_3N_2, which was subsequently hydrolyzed to produce NH_3 and regenerate MgO. However, the surface temperature of the Mg reached 550℃ during the reaction, which is close to the melting point of Mg metal (650℃) [96].The caused agglomeration of Mg limited the exposed surface area under illumination, resulting in an average ammonia production rate of only 1.67μmol $g^{-1}h^{-1}$. This necessitates further modifications to increase the melting point of the reduced AMN, thereby enhancing the effective surface area over repeated cycles.

N_2 Fixation:

$$3\,Mg + N_2 \rightarrow Mg_3N_2 \tag{21}$$

NH_3 Production:

$$Mg_3N_2 + 3H_2O \rightarrow 3MgO + 2NH_3 \tag{22}$$

Light-driven Reduction:

$$MgO + CH_4 \rightarrow Mg + 2H_2 + CO \tag{23}$$

Alkali and alkaline earth metal hydrides (AMH) exhibit high reactivity for nitrogen fixation, and the hydrogenation of AMN at low temperatures is thermodynamically favorable, positioning AMN as promising nitrogen carriers for H_2-CLAS [97]. Michalsky et al. [54] investigated the thermodynamics of AMN to AMH conversion. Experimental results showed that Ca_3N_2 and Sr_2N produced NH_3 at rates of 98 and 81 μmol $g^{-1}h^{-1}$ at 550℃ respectively, converting to Ca_2NH and SrH_2. They concluded that hydrogen could replace lattice nitrogen, thereby facilitating the low-temperature conversion of AMN to AMH and NH_3 production, with a high-temperature reduction of N_2 to regenerate AMN.

N_2 Fixation & Reduction:

$$6Ca_2NH + N_2 \rightarrow 4Ca_3N_2 + 3H_2 \tag{24}$$

NH_3 Fixation & Reduction:

$$2\,Ca_3N_2 + 3\,H_2 \rightarrow 3\,Ca_2NH + NH_3 \tag{25}$$

N_2 Fixation & Reduction:

$$4SrH_2 + N_2 \rightarrow 2Sr_2N + 4H_2 \tag{26}$$

NH_3 Production:

$$2\,Sr_2N + 7\,H_2 \rightarrow 4\,SrH_2 + 2\,NH_3 \tag{27}$$

Miyaoka et al. [85,98] studied Li_3N as a potential catalyst for ammonia synthesis under ambient conditions. By reacting with Group (14) elements (carbon, silicon, germanium, tin) to form lithium alloys, Li_3N can achieve nitrogen dissociation and recombination below 500℃ (Eqs. 28–30). Furthermore [99], they explored the use of Li_3N as a nitrogen carrier in direct hydrogenation to LiH for CLAS. Experimental results demonstrated that Li_3N could achieve the CLAS at 500℃ and 0.1 MPa. During the NH_3 production process, Li-Sn alloy exhibited excellent catalytic activity, achieving an ammonia production rate of over 120μmol $g^{-1}h^{-1}$ ammonia production in H_2 and N_2 mixtures at temperature as low as 150℃. However, the rate declined above 300℃ due to the overreaction of H_2 and N_2 on the catalyst surface, which competed for active sites. The high thermodynamic stability of Li alloys

Table 4
Thermodynamic properties of reactions between Li, N, and H[105].

Reactions	ΔH° 298 K (kJ/mol)	ΔS° 298 K (J/mol·K)	ΔG° 298 K (kJ/mol)
$6Li + N_2 \rightarrow 2Li_3N$	−394	−191.6	−336.9
$2Li + H_2 \rightarrow 2LiH$	−181	−130.7	−142.1
$2Li + 2NH_3 \rightarrow 2LiNH_2 + H_2$	−267.2	−254.9	−191.2
$Li_3N + H_2 \rightarrow LiH + Li_2NH$	−115.5	−130.7	−76.5
$Li_2NH + H_2 \rightarrow LiH + LiNH_2$	−48	−130.7	−9.1
$LiNH_2 + H_2 \rightarrow LiH + NH_3$	43.1	62.1	24.6
$Li_3N + NH_3 \rightarrow LiNH_2 + Li_2NH$	−158.6	−192.8	−101.2
$Li_3N + LiNH_2 \rightarrow 2Li_2NH$	−67.5	0	−67.5
$2LiNH_2 \rightarrow NH_3 + Li_2NH$	91.1	192.8	33.6
$4LiH + N_2 \rightarrow 2H_2 + 2Li_2NH$	−82	69.8	−102.8

necessitates a regeneration temperature of 500℃, prompting the exploration of alternative reaction pathways, potentially through thermochemical and electrochemical processes [100].

Reduction:

$$Li_yM + Li_zM + LiH \rightarrow Li_xM + H_2 \quad (28)$$

N_2 Fixation:

$$Li_xM + N_2 \rightarrow Li_yM + Li_3N \quad (29)$$

NH_3 Production:

$$Li_yM + Li_3N + H_2 \rightarrow Li_zM + LiH + NH_3 \quad (30)$$

M means the material from Group (14) elements.

Tang et al. [101] developed a liquid lithium-based alloy cycle system (Fig. 5). In this system, nitrogen reacts with a Li-Sn alloy at 510℃ to form Li_3N, and H_2 reacts with Li_3N dissolved in LiCl-KCl eutectic salt at 450℃ to form LiH and NH_3 will be produced. The reaction kinetics of H_2 with Li_3N in the molten salt are faster than in solid Li_3N, but the overall ammonia production rate was only 0.249μmol $g^{-1}h^{-1}$ due to the limited residence time of H_2 and N_2 in the liquid and incomplete lithium regeneration.

AMN presents significant potential for H_2-CLAS due to its favorable thermodynamics for nitrogen fixation and ammonia production. However, the thermodynamically challenging reduction and regeneration of the metal necessitates novel reaction pathways to overcome the high thermodynamic stability of AMH. Furthermore, metals such as Li, Mg, Ca, and Sr are highly reactive with H_2O in the air, posing safety risks. The high reactivity of AMN also makes them susceptible to oxidation by H_2O and O_2, which impedes regeneration. Therefore, ensuring safe storage and handling is crucial for industrial applications [41,64].

2.2. Alkali and alkaline earth metal imides as N carriers

2.2.1. Reactions of AMNH materials

In 2002, Chen et al. [102] discovered that Li_3N and Li_2NH could reversibly store hydrogen under mild conditions, exhibiting relatively high gravimetric capacity. They proposed a hydrogen storage material design strategy that utilizes both positive hydrogen (protons, H^+) and negative hydrogen (hydride ions, H^-). In this approach, the valence of hydrogen in AMH is −1, while in alkali metal or alkaline earth imide (AMNH), it is + 1. The combination of these materials releases gaseous hydrogen [103]. Furthermore, alkali metal and alkaline earth hydrides, nitrides, imides and amides can react with hydrogen and ammonia to shuttle hydrogen atoms between the −1 (hydride, H^-), 0 (H_2), and + 1 (imide and NH_3) valence states, as well as nitrogen atoms between −3 (nitride, N^{3-}), −2 (imide, HN^{2-}), −1 (amide, H_2N^-), and 0 (N_2) valence states [104,105].

Table 5
Kinetic parameters (activation energy and pre-exponential factor) for AMNH materials, calculated based on measurements from cited references.

Material	Nitrogenation		Hydrogenation		Ref.
	Activation energy, E_a (kJ mol^{-1})	Pre-exponential factor, ln(A) (ln (mol min^{-1} g^{-1}_{AMH}))	Activation energy, E_a (kJ mol^{-1})	Pre-exponential factor, ln(A) (ln (mol min^{-1} g^{-1}_{AMH}))	
LiH/Li_2NH	101.8	7.63	62.8	2.20	[87,92]
Mn_4N-LiH/Li_2NH	51.3	2.45	56.2	2.83	[92]
Zn-8LiH/Li_2NH	50.7	0.64	59.4	3.69	[87]
BaH_2/BaNH	96.0	8.75	41.5	0.53	[30]
Mn_4N-BaH_2/BaNH	52.3	2.13	36.2	−0.32	[92]
50 %Ni-BaH_2/BaNH	45.6	0.81	33.3	−0.19	[30]

The reactions between Li, N, and H are listed in Table 4. Inspired by the low-temperature (300–450℃) thermal decomposition of $LiNH_2$ which released NH_3 as a side reaction, Chen and co-workers utilized the excellent nitrogen fixation performance of AMH materials and the conversion between nitride and imide to develop a new H_2-CLAS process [30]. In this process, the hydride acts as a strong reducing agent to react with N_2, where the negative hydrogen ion (−1) is oxidized to form an imide (+1) and H_2 (0); subsequently, the imide reacts with H_2, where the hydrogen atoms of H_2 (0) disproportionate into hydride (−1) and NH_3 (+1). The main reactions are as follows, where *x* is the valence of M [9,106]:

N_2 Fixation:

$$4\,AMH_x + x\,N_2 \rightarrow 2x\,AM_{2/x}NH + x\,H_2 \quad (31)$$

NH_3 Production:

$$x\,AM_{2/x}NH + 2x\,H_2 \rightarrow 2\,AMH_x + x\,NH_3 \quad (32)$$

Compared to H_2O-CLAS, the nitrogen fixation and hydrogenation of metal nitrides in H_2-CLAS are less thermodynamically hindered but encounter significant kinetic barriers, resulting in low ammonia production rates at practical temperatures. In CLAS cycles, by utilizing the hydride-imide loop (AMNH-H_2-CLAS), the nitrogen fixation process does not involve the reduction of metals or metal nitrides. Instead, the metal hydride in the chemical loop provides both electrons for N_2 activation and protons to form the imide, rendering hydrogenation and nitridation thermodynamically favorable even at relatively low temperatures (300-500℃). Therefore, AMNH-mediated CLAS offers higher ammonia production rates and can operate under milder conditions compared to nitride-based loops. The reaction kinetics of several AMNH materials are summarized in Table 5.

The alkali metal amides $NaNH_2$ and KNH_2 exhibit favorable thermodynamics for hydrogenation at low temperatures, but they cannot form NaNH or KNH imides, making nitrogen fixation and reduction challenging [107]. CaNH and MgNH are unstable when heated, tending to convert to Ca_2NH (or Ca_3N_2) [108] and Mg_3N_2 [109] during nitrogen fixation, thus necessitating forcing operation in a MN-H_2-CLAS cycle. Consequently, overall ammonia efficiency is low. Chen et al. [35] found that, in conventional synthesis, adding AMH can enhance N_2 transfer on

Mn_2N catalysts, significantly improving N_2 activation and conversion to NH_3. The catalytic activity order of AMH is BaH_2 > LiH > KH > CaH_2 > NaH [40].

Many hydrogen vacancies exist in the bulk phase of BaH_2 which can effectively facilitate the nitrogen fixation reaction and form BaNH [110,111]. Chen et al. [30] compared the performance of BaNH, Li_2NH, and CaNH as CLAS nitrogen carriers. All three metal hydrides investigated reacted with N_2 to form the corresponding imide with BaH_2 and CaH_2, achieving the fastest reaction rates at 260℃. In the hydrogenation step, BaNH and Li_2NH reacted with H_2 at 200℃ to produce NH_3, whereas CaNH produced almost no NH_3 due to the formation of the byproducts Ca_2NH and Ca_3N_2 during nitrogen fixation. These calcium compounds required temperatures above 550℃ to react with H_2 and produce ammonia [54,92,111].

2.2.2. Improvements to AMNH materials: Catalysts and supports

By introducing nickel, the total ammonia production performance of BaNH and Li_2NH was enhanced, reaching 3125μmol $g^{-1}h^{-1}$ and 1530μmol $g^{-1}h^{-1}$, respectively. Kinetic analysis [110] shows that the synergistic effect of BaH_2 and Ni significantly reduces the activation energy for nitrogen fixation, lowering the required temperature by 150℃. Additionally, the introduction of carbon nanotubes (CNT) and Co metal [112] into the BaNH system resulted in an NH_3 production rate of over 20000μmol $g^{-1}h^{-1}$ at 10 bar and below 400℃, which is 2.5 times higher than the ammonia synthesis performance of traditional Ru-based catalysts. After studying Li_3N as a nitrogen carrier for H_2-CLAS, Miyaoka et al. [113] sought to avoid the high thermodynamic stability issues of regenerating Li from LiH. At 1 bar and 500℃, LiH reacted with N_2 to form Li_2NH and release H_2. Subsequently, the Li_2NH reacted with H_2 at 1 bar and 350℃ to produce NH_3. Thermodynamically, both nitrogen fixation and ammonia production processes are exothermic. Miyaoka et al. [113] found that for nitrogen fixation over LiH to form Li_2NH at 500℃, the rate of reaction gradually slowed down as Li_2NH began to agglomerate, hindering gas–solid reactions. Despite this, the conversion in AMNH-H_2-CLAS remained above 80 % after 1000 min under 0.1 MPa of N_2 flow. To address agglomeration, they introduced Li_2O scaffolds as support materials and controlled particle size to improve reaction kinetics. Chen et al. [114] also studied the chemical looping performance of Li_2NH, introducing zinc and nickel as co-catalysts. The LiH modified with Zn lowered the temperature required for nitrogen fixation to 350℃ and achieved an ammonia production rate of 956μmol $g^{-1}h^{-1}$. In the Li_2NH-mediated chemical loop, byproducts $LiNH_2$ and Li_3N coexist with Li_2NH, acting as nitrogen carriers which quickly reacted exothermically to form Li_2NH [114].

The development of the new AMNH-H_2-CLAS based process has advanced ammonia synthesis under ambient conditions. Compared to MN-CLAS requiring 500℃-1500℃, AMNH-CLAS leverages the good thermodynamic properties of AMNH to operate below 500℃. However, alkali metal and alkaline earth hydrides and imides can react rapidly with H_2O and O_2, forming oxides and hydroxides, which deactivate the nitrogen carriers and prevent regeneration. Therefore, further research on the long-term stability and recyclability of these nitrogen carriers and overall process safety measures are necessary. Furthermore, a sufficient understanding of the fundamental thermodynamics of imides, with regards to non-stoichiometry as a function of nitrogen partial pressure and temperature, is required for material improvement as well as the corresponding reactor and process design.

2.3. Thermodynamics of AMNH materials

The thermodynamics of AMNH or MN nitrogen carriers used for NH_3 production have a profound impact on ammonia production. From a computational model of ammonia production *via* chemical looping, Pereira et al. determined that, for MN-H_2-CLAS [37] and AMNH-H_2-CLAS [115], the equilibrium pN_2 of the solids formed during the nitrogenation step was a key parameter in terms of the overall efficiency, as the value of pN_2 determines the amount of nitrogen fixed during nitrogenation, and, equivalently, the maximum theoretical yield of ammonia at equilibrium. For materials with low pN_2 at equilibrium, the maximum theoretical yield of ammonia during hydrogenation is consequently low, as the hydrogenation reaction becomes thermodynamically limited, and decomposition of the ammonia product becomes favorable. To be competitive with the incumbent Haber-Bosch process, the authors determined that a per-pass ammonia yield of at least 26 % was required in each hydrogenation step at elevated pressure (150 bar), in order for the ammonia formed to be separated from the unreacted H_2 and N_2 by condensation [115]. By screening AMNH carriers (Li_2NH, MgNH, CaNH, SrNH, BaNH), based on available formation enthalpy and entropy data, LiH/Li_2NH was determined to be potentially feasible, with a maximum theoretical NH_3 yield of 63 % [115]. High-throughput screening [37] of mono- and bi-metallic MN materials identified 111 nitrides with sufficient theoretical ammonia yield at 150 bar – however, many computed thermodynamic properties lacked experimental verification. Moreover, although the MN-H_2-CLAS and AMNH-H_2-CLAS processes have been demonstrated to produce ammonia at ambient pressure, the authors concluded that if condensation was used to separate the ammonia from the process stream (as in the Haber-Bosch process), the net energy consumption was relatively insensitive to reactor operating pressure [115]. Therefore, to fully take advantage of CLAS at near-ambient pressure, novel techniques are needed for separating dilute ammonia from H_2 and N_2 at low pressure, such as selective membrane separation [116] or metal halide sorbents [117].

An additional complication for AMNH-H_2-CLAS arises from the interplay between different Li-N–H compounds and incomplete conversion of the hydride to the imide during nitrogenation. Makepeace and co-workers found that for solids containing Li, N, and H, prepared by solid-state synthesis [103] or reaction with N_2 gas [106], a wide range of compositions could form. Nitrogenation of LiH at 300–500 °C formed a partially converted imide of the form $Li_{2+x}NH$ ($0 < x < 2$), composed of a solid solution of Li_2NH (imide) and Li_4NH (described as 'hydride-nitride') [103]. The 'hydride-nitride' Li_4NH also underwent further nitrogenation, at an order of magnitude faster rate than LiH under equivalent conditions [106], to form imide and nitride products, as given in Eq. (33).. The 'hydride-nitride' Li_4NH also underwent further nitrogenation, at an order of magnitude faster rate than LiH under equivalent conditions [106], to form imide and nitride products, as given in Eq. (33).

$$3\,Li_4NH + N_2 \rightarrow 3\,Li_2NH + 2\,Li_3N \quad (33)$$

However, the factors influencing the conversion of LiH to $Li_{2+x}NH$, and hence, the maximum theoretical ammonia yield during hydrogenation, are not fully understood.

For BaH_2, another promising nitrogen carrier for AMNH-H_2-CLAS, less is known regarding the possible Ba-N–H-containing phases and their thermodynamics. However, from molecular dynamics simulations, Gardini et al. [118] postulated that BaH_2 reacts with N_2 to form the non-stoichiometric compound $BaH_{(2-2x)}(NH)_x$, with $0 < x < 1$. Experimental verification is needed to confirm the existence of the hypothesized $BaH_{(2-2x)}(NH)_x$ phase and determine the optimal conditions to maximize total nitrogen fixation. Hence, the extent to which process models can be developed for AMNH-H_2-CLAS systems with realistic nitrogenation of the AMNH nitrogen carrier is still limited, due to insufficient understanding of the thermodynamics.

3. Fabrication of N carriers

In addition to developing materials for CLAS with favorable kinetics and thermodynamics, the implementation of CLAS at an industrial scale requires the scale production of nitrogen carrier materials. Particular consideration has been given to the composition and morphology of these materials, as well as to structural changes that occur during the

Table 6
The synthesis methods of metal nitrides in CLAS.

Synthesis Method	Metal Nitride	Raw Materials	Atm	Temperature (℃)	Reference
Nitridation-Carbon Reduction	AlN	Al_2O_3	N_2, C	1700	[38]
	AlN	Al_2O_3, Y_2O_3	N_2, CH_4	800	[124]
	$MnN_{x-\delta}$	Mn, MnN_x	N_2, CH_4	750–1200	[53]
	Cr_2N	Cr, Cr_2O_3	N_2, H_2/CO	1000	[125]
	Mg_3N_2	Mg, MgO	N_2, CH_4	1500	[52,132,133]
Co-precipitation-Nitridation-Carbon Reduction	Si-AlN	$Al(NO_3)_3{\cdot}9H_2O$, $(NH_4)_2CO_3$, TEOS, C	Ar, N_2	1000, 1200	[77]
Molten salt synthesis	Mn_3N_2	Mn_2O_3, $NaNH_2$	N_2	240	[57]
Co-precipitation	Li-MnNx-δ	Li, Mn_3N_2, NH_4OH	Air	800	[57]
	Mo_2N	$(NH_4)_6Mo_7O_{24}{\cdot}4H_2O$, $C_6H_{12}N_4$	Ar	600	[58]
Nitridation	$Mn_6N_{2.58}$	Mn	N_2	700–750	[54]
	Ca_3N_2	Ca	N_2	750	[54]
	Sr_2N	Sr	N_2	750	[54]
	Sn-LiN_3	Li, Sn	N_2	500	[85]
Ammonolysis	Cu_3N	CuF_2	NH_3	300	[56]
	Ni_3N	$NiCl_2$	NH_3	480	[56]
	Zn_3N_2	Zn	NH_3	600	[56]
	Ta_3N_5	Ta_2O_5	NH_3	900	[56]
	Fe_3N_2	Fe	NH_3	500	[55]
	Co_2N	Co_3O_4	NH_3	700	[55]
	Re_3N	NH_4ReO_4	NH_3	350	[55]
	$CoRe_4N$	NH_4ReO_4, $Co(NO_3)_2{\cdot}6H_2O$	NH_3	700	[55]
	Co_3Mo_3N	$(NH_4)_6Mo_7O_{24}{\cdot}4H_2O$, $Co(NO_3)_2{\cdot}6H_2O$	NH_3, N_2	800	[59]
	Ni_2Mo_3N	$Ni(NO_3)_2{\cdot}6H_2O$, $Na_2MoO_4{\cdot}(H_2O)_2$	NH_3, N_2	700	[59]
	Co_3ZnN	$Co(NO_3)_2{\cdot}6H_2O$, $Zn(NO_3)_2{\cdot}6H_2O$, HNO_3	NH_3, N_2	400	[83]

chemical looping process [119]. The synthesis methods used to produce nitrogen carriers can influence the thermodynamic and kinetic properties of materials [28], thereby improving ammonia production rates and cyclability of nitrogen carriers, facilitating their potential industrial applications.

3.1. Preparation of MN as N carriers

3.1.1. Direct nitridation

Direct nitridation involves treating metals or metal oxides with nitrogen at high temperatures to produce nitrides [37,53,120]. Most nitrides can be synthesized by nitriding metal powders in a high-temperature nitrogen atmosphere. Reduced metals, particularly alkali metals and alkaline earths, are difficult and costly to transport due to their highly exothermic reactions with oxygen in air. Consequently, these metals are typically produced via the carbothermal or methane reduction of metal oxides [121], where *R* is a reducing agent (*e.g.* CO or CH_4), as illustrated in Eqs. 33–35.

N_2 Fixation:

$$a/bM + 1/2N_2 \rightarrow 1/bM_aN_b \quad (33)$$

NH_3 Production:

$$1/bM_aN_b + ad/bcH_2 \rightarrow a/bcM_cO_d + NH_3 + (ad/bc - 3/2)H_2 \quad (34)$$

Reduction:

$$a/bcM_cO_d + ad/bcR \rightarrow a/bM + ad/bcRO \quad (35)$$

Steinfeld et al. [38,39] employed carbothermal reduction of Al_2O_3 for CLAS by mixing activated carbon and Al_2O_3 at a C/Al_2O_3 molar ratio of 6:1 under 0.1 L/min N_2 at 1500-1700℃, reducing Al_2O_3 to AlN for hydrolytic ammonia production. However, as can be seen, the reduction required very high temperatures, up to 2000℃, resulting in forming inactive byproducts, including Al_2OC and Al_4C_3. Approaches have been made to reduce the temperature, it was found that catalysts such as Y_2O_3, Yb_2O_3, and Cr_2O_3 could lower the minimum temperature required to reduce Al_2O_3 [122]. Zhang et al. [123] mixed Al_2O_3, C, and Y_2O_3 at a molar ratio of 3:3:0.03, using Y_2O_3 as a catalyst to convert high-melting-point Al_2O_3 (1800℃) into lower-melting-point aluminum compounds (1450℃). The reactions between the Al-Y-O compounds and C are liquid–solid reactions instead of solid–solid, resulting in more rapid kinetics of nitride formation and allowing for nitridation at 1200℃-1500℃ [124]. Alternatively, the reduction of Al_2O_3 in CH_4 has more rapid kinetics than reduction with C. Fu et al. [125] discovered through thermodynamic analysis that Al_2O_3 could be converted to AlN at 1135℃ using CH_4 as a reducing agent. The introduction of V_2O_3 further decreased the reduction temperature to 778℃. Pfromm et al. [62] utilized CH_4 as a reducing agent to produce Mn nitrogen carriers in the H_2O-MN-CLAS. In the nitridation process, CH_4 alongside N_2 facilitates the conversion of MnO to $Mn_6N_{2.58}$. However, the required temperature remained at 1150℃. This high temperature is due to the decomposition of CH_4 throughout the process, exacerbated by the formation of CO and H_2 during the by-product Mn_7C_3 formulation. Consequently, the overall conversion efficiency was only 38 % [54]. Miyaoka et al. [100] demonstrated it is feasible to synthesize AMNs such as Li_3N through the direct reaction of metals with N_2 under moderate conditions. The active propensity of Li which enables its nitrogen fixations at ambient temperature is attributed to the low dissociation energy barrier of N_2 on the Li surface.

3.1.2. Ammonolysis

While the direct nitridation method for preparing transition metal nitrides is straightforward, the nonpolar triple bonds in nitrogen are difficult to break, requiring an activation energy of 940.95 kJ/mol. Consequently, high temperatures are often required for the nitridation process [120]. The ammonolysis method, which employs NH_3 to reduce metal oxides and replace oxygen atoms with nitrogen, is a primary technique for synthesizing transition metal nitrides. Hargreaves et al. [126] synthesized Mo nitrides from MoO_3 by ammonolysis, converting 1 g of MoO_3 under a 94 ml/min NH_3 flow and 785℃ to Mo_2N. Khalifah et al. [127] produced Co_3Mo_3N by annealing $CoMoO_4$ under a 50 ml/min NH_3 at 750℃ for 12 h. Higher NH_3 flow rates and lower heating rates can mitigate steam-induced sintering during heating. However, during ammonolysis, a certain fraction of the ammonia used decomposes to H_2 and N_2 due to the elevated temperatures used, decreasing the overall efficiency. This issue can be mitigated by increasing the NH_3 flow rate and reducing the heating rate [128,129]. Furthermore, metals which react with ammonia to form a metal nitride are also likely to be favorable for catalyzing decomposition of NH_3 [37,130], meaning that not all nitride materials produced by ammonolysis will be suitable for CLAS. Recently, Yun et al. [131] demonstrated that the ammonolysis of $Ti_{1-x}Ru_xO_2$ led to the exsolution of Ru

Table 7
Two ways to generate metal hydrides for CLAS.

Synthesis Method	Raw Materials	Atmosphere	Products	Temperature	Pressure
Hydrogenation	Ba, Li, Ca	H_2	Hydride	400 ℃	20 bar
Amidation	Ba, Li, K	NH_3, H_2	Amide, Hydride	200 ℃	10 bar

nanoparticles embedded within a TiN matrix, significantly enhancing the catalytic activity for electrocatalysis. This process was carried out at 900℃ under an NH_3 flow, resulting in the selective nitridation of titanium without the formation of any ruthenium nitride phases, highlighting the specificity of titanium nitridation. The exsolved Ru nanoparticles exhibited excellent electrocatalytic performance, which was attributed to their strong interaction with the TiN matrix and enhanced electron transfer capabilities. This approach presents an important strategy for the future design and synthesis of efficient ammonia synthesis catalysts or nitrogen carriers.

The synthesis methods of metal nitrides in CLAS are summarized in Table 6. Direct nitridation is suitable for industrial applications due to its simplicity, clear reaction pathways, and economical equipment. Considering the slow nitridation kinetics of metals, high-pressure, high-temperature operations and appropriate catalysts are needed at the current stage [27,36].

3.2. Preparation of AMNH as N carriers

In AMNH-H_2-CLAS processes, AMNH materials are produced by nitridation of alkali metal or alkaline earth hydrides. However, due to the high costs and risks of oxidation during transport, these hydrides can be prepared from metal *via* high-pressure hydrogenation and metal amidation [86,112]. The synthesis methods of metal nitrides in CLAS are summarized in Table 7. Chen et al. [30] compared the performance of BaNH, Li_2NH, and CaNH in CLAS with AMNH synthesized by reacting AMH with N_2. Specially, BaH_2 was synthesized by hydrogenating Ba metal under 20 bar H_2 and room temperature for two days, followed by heat treatment at 400℃ under 10 bar H_2 for 3 h:

Hydrogenation:

$$AM + x/2H_2 \rightarrow AMH_x \tag{36}$$

Amidation involves reacting an alkali metal or alkaline earth with NH_3 to form a metal amide, which can then react with H_2 to produce an imide. Chen et al. [134] investigated the hydrogenation reactions of $LiNH_2$, KNH_2, and $Ba(NH_2)_2$ for ammonia production, KNH_2 and Ba $(NH_2)_2$ were synthesized by reacting K and Ba metals in a 99.999 % NH_3 atmosphere under room temperature and 7 bar pressure for two days [92,135]. Subsequently, $AMNH_2$ was converted to LiH, KH, and BaH_2 under 10 bar H_2 and 240-340℃ ($LiNH_2$), 80-180℃ (KNH_2), as well as 130-230℃ ($Ba(NH_2)_2$). Compared to the hydrogenation method, the imide method first converts metals to metal imides under lower pressure, followed by hydrogenation and heating to produce metal hydrides [30,134]. The reactions are expressed in Eqs. 37–38.

Amidation:

$$AM + xNH_3 \rightarrow AM(NH_2)_x + x/2H_2 \tag{37}$$

Hydrogenation:

$$AM(NH_2)_x + xH_2 \rightarrow AMH_x + xNH_3 \tag{38}$$

For CLAS utilizing AMNH as nitrogen carriers, the key lies in preparing the hydride which can then react with N_2 to form AMNH for subsequent hydrogenation to produce ammonia. Compared to amidation, direct hydrogenation is simpler, requiring fewer materials and equipment, making it more suitable for large-scale applications. However, direct hydrogenation has slower reaction kinetics, requiring higher pressures and longer times, necessitating increased temperatures or adding catalysts such as TM and MgO [110,112].

3.3. Improvement

For continuous CLAS, the synthesis and regeneration of MN and AMNH needs to be economically feasible. Direct nitridation and hydrogenation of metal elements are more simplified and suitable for large-scale synthesis. To improve these, material modification is crucial. Ideal nitrogen carriers should exhibit high nitrogen fixation and ammonia production efficiency, strong mechanical strength, stability over repeated cycles, low preparation cost, and should be environmentally friendly. Main modification methods include using catalysts, compositing, geometry control, and external field-assisted techniques.

3.3.1. Catalytic promotion

Single metal nitrides are normally too stable to be reduced by hydrogen at mild temperatures (<800℃), or have slow rates of nitrogen fixation, hindering regeneration. Doping the nitrogen carrier materials with promoters or compositing to improve reaction kinetics is a common modification method to increase the rates of nitrogen fixation and/or hydrogenation. Introducing suitable promoters into nitrogen carriers to accelerate reaction processes is another approach. Liu et al. [44,136] found that TiO_2 and Fe_2O_3 doped AlN significantly reduced activation energy for hydrolytic ammonia production and provided hydroxyl groups for nitrogen desorption, improving NH_3 production. Pfromm et al. [62] mixed NaOH with Mn nitride, where Na cations acted as electronic promoters, weakening Mn-N bonds, reducing lattice nitrogen stability. As a result, the hydrolytic ammonia yield increased from 4 mol % to 54 mol%. Pfromm et al. [60] used $CaO/Ca(OH)_2$ to increase the concentration of Lewis acid sites in Cr_2N, which resulted in the release of more NH_3 during the hydrolysis of Cr nitride (1.56 times).

Transition metals (TM) with relatively weak nitrogen binding strength can serve as lattice nitrogen reactivity regulators. Density functional theory (DFT) analysis of TMN lattice geometry and electronic structure revealed that lattice nitrogen stability in TMN could be altered by doping with transition metals such as Cr, Fe, Co, Ni, and Mo [82,137,138]. Compared to single metal nitride [139], doping with multi-metal nitrides reduces nitrogen fixation conditions and accelerates reactions by increasing nitrogen vacancy concentrations, promoting the fixation and transfer of lattice nitrogen [140]. Michalsky et al. [53] mixed Mo-Cr and Mn-Fe metal powders, and nitrided them at 750℃. The doped nitrides reacted with water at 500℃ to produce ammonia, significantly lowering the temperature required for ammonia production. Investigations combining electronic structure computations with experimental studies. Compared to single metal nitride [139], doping with multi-metal nitrides reduces nitrogen fixation conditions and accelerates reactions by increasing nitrogen vacancy concentrations, promoting the fixation and transfer of lattice nitrogen [140]. Michalsky et al. [53] mixed Mo-Cr and Mn-Fe metal powders, and nitrided them at 750℃. The doped nitrides reacted with water at 500℃ to produce ammonia, significantly lowering the temperature required for ammonia production. Investigations combining electronic structure computations with experimental studies [52,54] have shown that the introduction of Cr and Fe leads to the efficient disruption of lattice nitrogen, thereby decreasing the binding affinity and facilitating the transfer of lattice nitrogen. Nevertheless, a portion of lattice nitrogen is liberated in the form of N_2, which in turn has implications on the rates of NH_3 conversion [57,141]. Ball milling (Eqs. (39) and chemical reduction methods (Eqs. (40a) and (40b) were used to prepare Pd-Li-H composites composed of Pd metal, $PdH_{0.7}$, and LiH, with the Pd enhancing the reaction activity of LiH/Li_2NH [86]. The presence of Pd promoted nitrogen

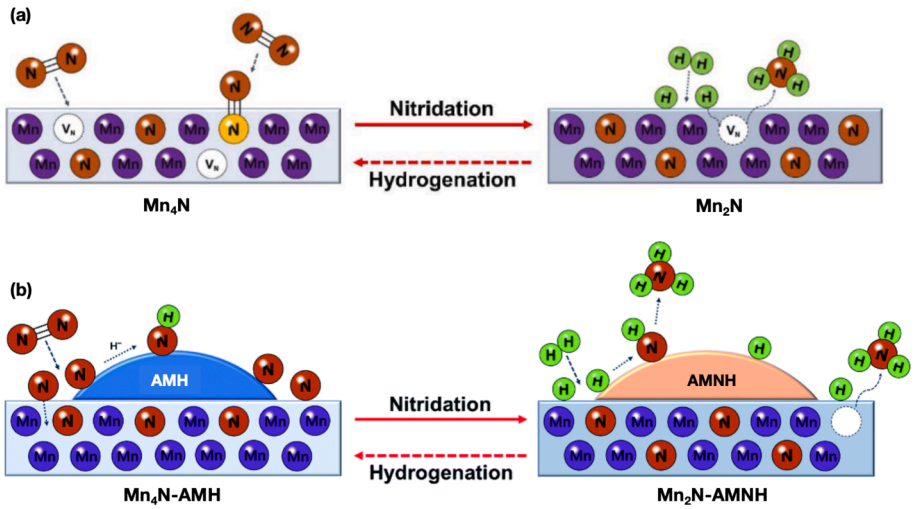


Fig. 6. Schematic diagram of CLAS mediated by (a) Mn_4N/Mn_2N and (b) Mn_4N-AMH/Mn_2N-AMNH [92]. Copyright 2021 Royal Society of Chemistry.

fixation on LiH and hydrogenation of the resulting Li_2NH, increasing catalytic activity sevenfold compared to pure LiH, with an ammonia production rate of 693μmol $g^{-1}h^{-1}$ at 300℃ and 1 bar. Ball milling (Eqs. (39) and chemical reduction methods (Eqs. (40a) and (40b) were used to prepare Pd-Li-H composites composed of Pd metal, $PdH_{0.7}$, and LiH, with the Pd enhancing the reaction activity of LiH/Li_2NH [86]. The presence of Pd promoted nitrogen fixation on LiH and hydrogenation of the resulting Li_2NH, increasing catalytic activity sevenfold compared to pure LiH, with an ammonia production rate of 693μmol $g^{-1}h^{-1}$ at 300℃ and 1 bar. Chen et al. [90] summarized the TM promotion sequence for LiH: Co ≈ Fe ≥ Cr ≈ Mn > Pd > V > Ni.

Ball milling:

$$Pd + LiH \rightarrow Pd_LiH \tag{39}$$

Hydrogenation:

$$PdCl_2 + 3LiH \rightarrow Pd \bullet LiH + 2LiCl + H_2 \tag{40a}$$

$$PdCl_2 + 2LiH \rightarrow PdH_{0.7} + 2LiCl + 1.3/2H_2 \tag{40b}$$

Doping with AM has the potential to enhance the reaction kinetics involving lattice N and H atoms within nitrogen carriers. In their research, Hargreaves et al. [141] found that doping with Mg nitrides with lithium doping altered the bulk and surface structure of the nitrogen carrier. In the case of doping of Mn nitrides, the introduction of Fe may diminish the stability of crystal lattice N within Mn nitride. However, the capability for activation and dissociation of H_2 molecules remains limited. Doping with Li can mitigate the formation of nitrogen vacancies, thereby facilitating the dissociation and adsorption of H_2 molecules, which leads to an enhancement in the rate of generation and conversion of NH_3 during the process of releasing lattice N. Hence, AM dopants have the potential to enhance the thermodynamic properties of nitrogen carriers by diminishing the energy required for N vacancy formation, facilitating the collision at the surface between N and H species to form ammonia.

Composites composed of multiple different metal nitrides with specific crystal structures can improve the kinetics of nitrogen fixation and ammonia production, as a result of synergistic effects between different cations in the material. Ye et al. [14] mixed $Ni(C_5H_5)_2$ with LaN under H_2 flow at 250℃ for 1.5 h to obtain Ni-LaN composite nitrogen carriers. Nitrogen vacancies on the LaN surface were confirmed from DFT calculation to weaken N≡N bonds, activating N_2, while Ni on LaN surface dissociates H_2, promoting nitrogen binding and releasing NH_3 and new nitrogen vacancies. This synergy increased the ammonia production rate from nearly zero to 5543μmol $g^{-1}h^{-1}$at 400℃ and 1 bar for the Ni-LaN composite. Chen et al. [92] designed multifunctional Mn_4N with LiH or BaH_2 composites (Fig. 6), with nitrogen carriers mutually acting as catalysts, improving each other's reaction kinetics. Mg nitride acted as nitrogen carrier and catalyzed LiH or BaH_2 nitrogen fixation and ammonia production kinetics, while LiH or BaH_2 promoted the interconversion of N-poor and N-rich Mn nitride. The rate of ammonia production for the composite system was an order of magnitude higher than for pure AMNH and MN-mediated CLAS, reaching 1576μmol $g^{-1}h^{-1}$ at 300℃ and 1 bar.

3.3.2. *Structural modification*

Designing nitrogen carrier structures to increase reaction sites and enhance reaction kinetics is another research direction in modifying nitrogen carriers. This involves controlling material particle size and structure or loading nitrogen carriers onto high-surface-area supports. Reduction in particle size adjusts the surface structure of nitrogen carriers and influences the number of active sites [142]. As found in ball milling and reduction method comparison [86], reduction-produced materials had smaller particle sizes with larger specific surface area [143], increasing surface active sites for N_2 and H_2 contact.

Miyaoka et al. [113] mixed Li_2O with LiH as a scaffold, by dispersing Li_2NH in Li_2O matrix to prevent agglomeration, Li_2NH particle size was reduced, and reaction kinetics were improved. Chen et al. [91] found that lower iron loadings led to smaller Fe particles (1.70 nm), which increased surface area contact with adjacent LiH and enhanced the NH_3 production rate by 9 times (74000 μmol $g_{Fe}^{-1}h^{-1}$). The surface area available for reaction, and the stability of nitrogen carriers over repeated cycles, can be optimized by producing materials with porous structures [113]. Qin et al. [144] synthesized foamy porous (Al_2O_3 + C) precursors using low-temperature combustion with aluminum nitrate, urea, glucose, and carbothermal reduction which are to produce AlN powders. Foamy porous structures significantly decreased reduction temperatures and produced fine and well-dispersed AlN powders. Wu et al. [123]used carbothermal reduction to create porous aluminium-based nitrogen carriers, it was reported excess Al_2O_3 increased carrier porosity and enhanced nitrogen desorption. Pfromm et al. [60] dispersed chromium nitride on high-surface-area quartz wool to increase reaction sites and promote nitrogen protonation. The findings displayed that the augmentation in reaction surface area allowed NH_3 to be removed from the surface rapidly, this decreased the extent of decomposition to N_2 and H_2 and thereby boosted the rate of ammonia formation by a factor of ~ 2.6. Wu et al. [77] synthesized Si-modified Al_2O_3 composites using coprecipitation. Compared to single Al nitrogen carriers, these composites exhibited greater resistance to high-temperature phase transitions and pore structure collapse with longer cycles.

Table 8
Different modification methods of CLAS materials.

Type	Method	Detail	Example				Ref.
			Original	Modification	Ammonia production rate (μmol $g^{-1}h^{-1}$)		
					Original	Modification	
Catalysis promotion	Doping	Add catalysts or promoter to enhance reaction kinetics and thermodynamics	$Mn_6N_{2.58}$	NaOH-$Mn_6N_{2.58}$	229	3239	[62]
			Li_2NH	Pd-Li_2NH	100	693	[86]
	Compositing	Combine systems by synergistic effect to enhance reaction kinetics and thermodynamics	Ni, LaN	Ni-LaN	0, 0	5543	[14]
			Mn_2N, Li_2NH	Mn_2N-Li_2NH	50, 100	1576	[92]
Structural modification	Reduction of Particle size	Adjust catalyst surface structure and influence active sites	Ball-milling Pd-Li_2NH	Ball-milling reaction Pd-Li_2NH	458	596	[86]
			Ni-LaN bulk	Ni-LaN nanoparticle	2400	5543	[14]
	Porous	Increase material porosity to enhance gas desorption	Ni-BaNH	Al_2O_3-Ni-BaNH	1200	2770	[30]
			Ni-BaNH	MgO-Ni-BaNH	1200	3125	[30]

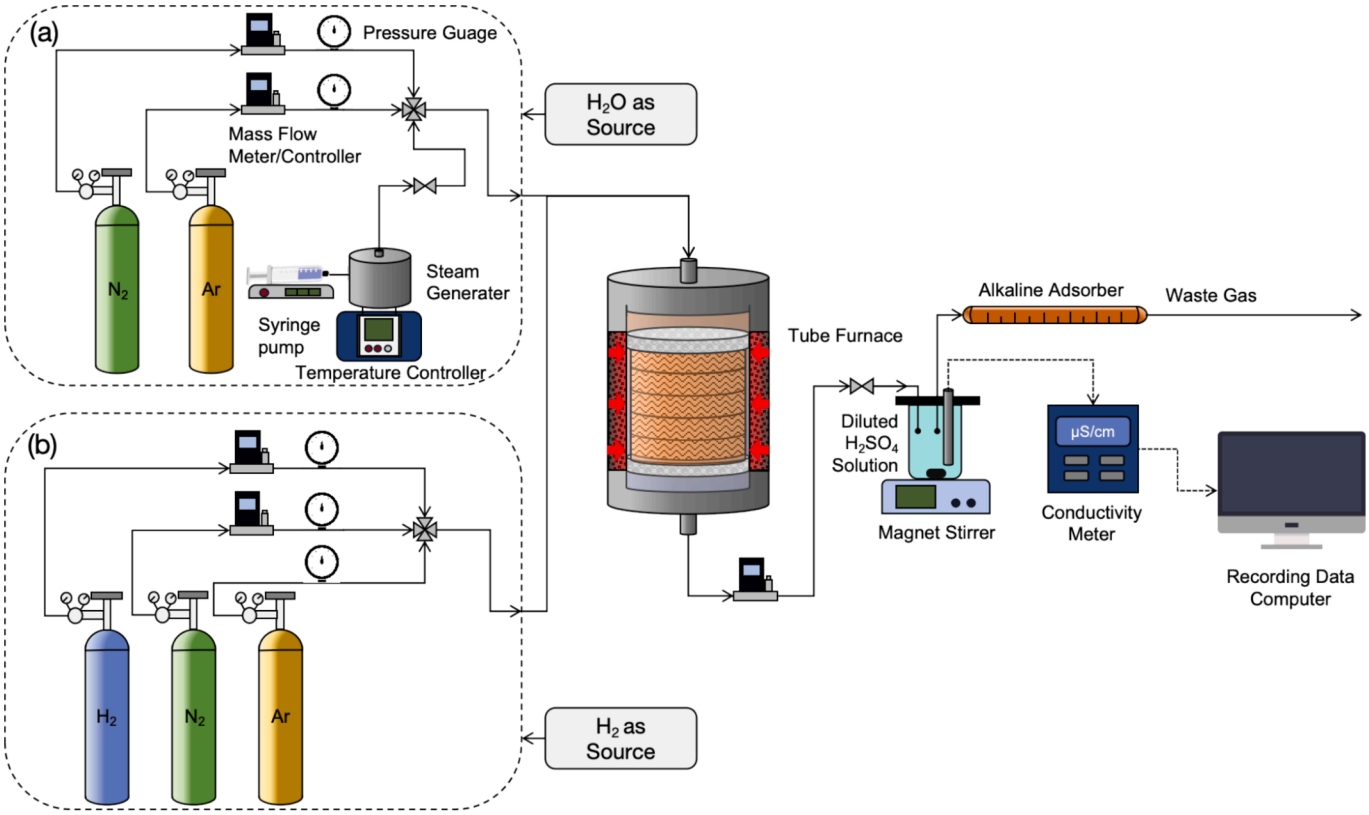


Fig. 7. Schematic diagram of the fixed-bed reactor-based CLAS for (a) H_2O-CLAS, (b) H_2-CLAS.

Loading nitrogen carriers onto high-surface-area supports to disperse promoters and improve reaction kinetics is another strategy for structural modification. Chen et al. [112] used carbon nanotubes (CNT) as a support to increase Co dispersion in Co-BaH_2 composites, significantly enhancing ammonia production efficiency. For Ni-BaH_2 materials, composites were preferably loaded onto Al_2O_3 using impregnation [145]. Impregnating Ni-Al_2O_3 mixing with Ba in liquid ammonia, followed by hydrogenation, produced Ni-BaH_2-Al_2O_3 materials. Results showed uniform Ba and Ni dispersion on Al_2O_3 doubled ammonia production rate (2770μmol $g^{-1}h^{-1}$ at 250°C and 1 bar). Besides, the materials produced ammonia under mild conditions (100°C and 1 bar). The different modification methods are summarized in Table 8. In addition to reactive performance, further considerations regarding the design of novel nitrogen carrier materials should include the toxicity of raw materials, mechanical properties, the feasibility of large-scale synthesis, and processes for recycling nitrogen carrier materials.

4. Reactors for CLAS systems

Currently, most experimental setups use fixed-bed reactors at lab-scale, with the main difference being the hydrogen source (H_2 or H_2O). For MN-H_2O-CLAS, Wu et al. [123] developed an AlN fixed-bed reactor for nitrogen adsorption/desorption, with hydrogen sourced from a steam generator. This reactor operates continuously at 1500 °C, enabling effective hydrolysis of AlN to produce ammonia, which is then collected and measured through titration. However, this method cannot continuously monitor ammonia production in real time. Additionally, the oxides produced from hydrolysis require further regeneration using reductants, which are highly energy-intensive, making it unsuitable for fixed-bed reactors. Yu et al. [58] developed a Mo_2N fixed-bed reactor for MN-H_2-CLAS. This apparatus can prepare molybdenum-based nanocomposites (by drying in an Ar atmosphere and passivating with 1 % O_2), as well as performing nitrogen fixation and hydrogenation of Mo_2N to produce ammonia. The reactor's outlet leads to a diluted sulfuric acid

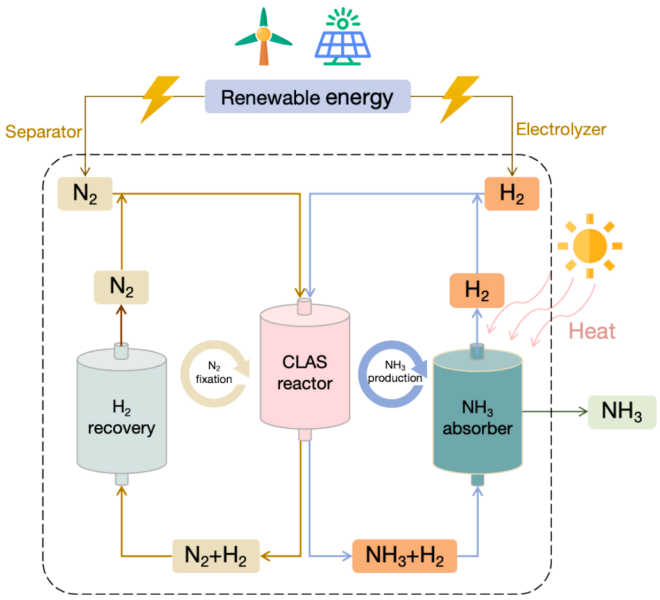


Fig. 8. The proposed setup contains a fixed-bed reactor for AMNH-CLAS and two fixed-bed reactors for separating NH_3 and waste H_2 [30].

solution, and the performance is measured in real-time using a conductivity meter, allowing for timely adjustments to furnace temperature and gas flow rates, thus enhancing operational control. Before nitrogen fixation and hydrogenation, the materials are passivated with 1 % O_2 and Ar, ensuring more precise performance measurements. The structure of the fixed-bed reactor-based H_2O-CLAS and H_2-CLAS is shown in Fig. 7.

For AMNH, Chen et al. [30,86,92] developed a quartz-lined stainless steel fixed-bed reactor to test nitrogen fixation and hydrogenation of LiH and BaH_2. They proposed a future multi-reactor coupling system (Fig. 8), where the main reactor performs CLAS, and two auxiliary reactors separately recover H_2 and NH_3 produced during the process. This design aims to address the issues of gas separation and excess hydrogen waste in CLAS.

4.1. Reactor improvements

Although fixed-bed reactors are widely used, CLAS requires more efficient and energy-saving reactor configurations. Circulating fluidized bed (CFB) and moving bed reactors are considered suitable for CLAS due to their excellent gas–solid contact properties and efficient heat and mass transfer [146]. These reactors enable continuous operation and can perform reactions under milder conditions, reducing energy consumption. CFB reactors ensure uniform temperature distribution and adequate gas–solid contact through the continuous circulation of solid particles, which is crucial for managing the endothermic and exothermic reactions in CLAS. Moving bed reactors, on the other hand, provide a stable reaction environment and reduced pressure drop through the continuous movement of solid particles, making them suitable for large-scale ammonia synthesis applications. In the future, incorporating advanced control systems and real-time monitoring technologies can further optimize reactor performance, ensuring stable production rates and high efficiency. Additionally, integrating regenerative heating systems can improve energy efficiency and reduce operational costs.

4.2. External field-assisted reactor

To further enhance ammonia production performance and improve energy consumption performance of CLAS, external field-assisted technologies, such as electro-driven [88,95,100], light-driven [52,53,80], and plasma-assisted [23,24,89], can be explored. These technologies can accelerate mass transfer and reaction rates, decrease the required temperatures and pressures for reactions. In Li-mediated CLAS development, electro-driven methods solved some thermodynamically unfavorable reduction or ammonia production reactions, enabling CLAS under milder conditions [95]. Chen et al. [88] developed a LiCl-NaCl-KCl eutectic electrolysis cell with nickel foam electrodes, demonstrating the feasibility of Li_2NH-mediated electro-driven CLAS (Fig. 9a). Electric input promoted both LiH nitrogen fixation and Li_2NH hydrogenation reactions, increasing the ammonia production rate eightfold (2058μmol $g^{-1}h^{-1}$) and reducing energy consumption (10.5 kWh kg^{-1}).

Swearer et al. [80] utilized light and plasma-driven catalysts to decrease reduction temperatures. Plasmonic TiN nanoparticles absorbed optical illumination, acting as photothermal antennas to provide reaction heat, which significantly reduced energy consumption. TiN-MgO composites were reduced by CH_4 to Mg metal, then reacted with N_2 to form Mg_3N_2 for hydrolytic ammonia production. Plasma catalysts induced localized heating and high-energy hot carriers, increasing reactant activity, which addressed MgO reduction's thermodynamic challenges and enhanced energy conversion efficiency, offering a novel industrial CLAS pathway. Introducing plasma pretreatment can further improve the process [84]. Plasma-treated preactivates stable N_2 molecules before they reach the surface of particles, enhancing surface reactivity during nitrogen fixation. This combination of microwave heating and plasma pretreatment effectively boosts the efficiency and speed of the nitrogen fixation process. Chen et al. [89] developed a plasma-driven CLAS reactor, as shown Fig. 9b. NaH does not react with N_2 under normal thermal conditions. However, nitrogen plasma can generate reactive nitrogen species and induce NaH dehydrogenation, forming $NaNH_2$, which is used for subsequent hydrogenation to produce ammonia at a rate of 550 μmol $g^{-1}h^{-1}$. By compositing NaH with MgO as support through ball milling, the ammonia synthesis rate of the plasma-driven CLAS reactor was further enhanced to 2080μmol $g^{-1}h^{-1}$. Performance summaries of different external field-assisted reactor in CLAS are given in Table 9.

5. Challenges

Despite the promising potential of Chemical Looping Ammonia Synthesis (CLAS) as an alternative to the Haber-Bosch process, several challenges still hinder its practical and industrial-scale application. These challenges span across material performance, reaction mechanisms, reactor design, and process scalability. Table 10 provides a comprehensive comparison of different CLAS routes and the Haber-Bosch process for ammonia synthesis, summarizing their respective advantages and limitations.

Low Ammonia Production Rates: Current nitrogen carriers, including transition metal nitrides (MNs) and alkali/alkaline earth metal imides (AMNHs), suffer from insufficient ammonia production rates compared to the Haber-Bosch process. Optimizing the catalytic pathways and nitrogen fixation mechanisms is necessary to enhance ammonia production rates.

Nitrogen Carrier Stability: The stability of nitrogen carriers over multiple reaction cycles is a critical limitation. For example, MNs exhibit promising initial activity, but high-temperature steam in H_2O-CLAS causes particle agglomeration, reducing long-term performance. Similarly, imide-based systems suffer from deactivation due to the formation of oxides when reacting with impurities such as H_2O and O_2. Addressing the degradation of carrier materials and improving their recyclability is essential for the sustained operation of CLAS.

Material Cost and Scalability: Many of the high-performance nitrogen carriers, especially those based on rare or expensive materials, face significant cost barriers for large-scale application. The economic feasibility of CLAS will depend on the development of cost-effective carriers that can maintain high performance under industrial conditions. Additionally, the sensitivity of AMNH materials to air and

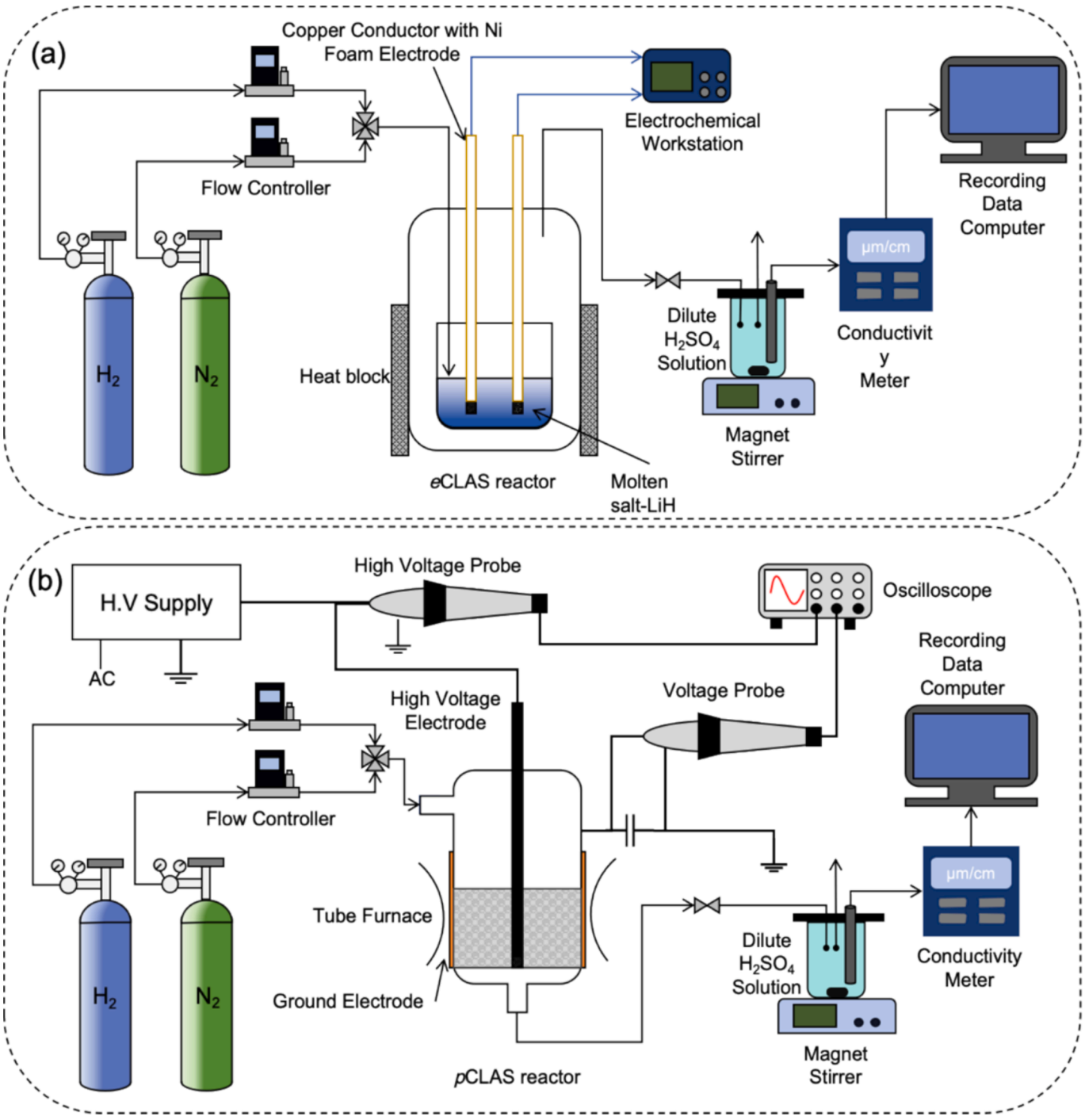


Fig. 9. Schematic of the experimental setup for (a) electro-driven CLAS, (b) plasma-driven CLAS.

moisture complicates storage and handling on a large scale, introducing further cost and safety concerns.

Characterization of Intermediates: One of the technical challenges in CLAS is the real-time characterization of nitrogen carrier intermediates under reaction conditions. Understanding the dynamic evolution of the carrier's chemical state and surface structure during the reaction is crucial to optimize the process. Current methods struggle to provide detailed insights into the active sites and intermediate species, limiting our understanding of the reaction mechanisms. More advanced techniques, possibly aided by molecular dynamics (MD) simulations and reaction kinetics modeling, are needed to bridge this gap.

Reactor Design: While reactors for chemical looping combustion are well established, the design of CLAS reactors is still in its infancy. Existing systems rely heavily on fixed-bed reactors for small-scale experiments, which limits the process efficiency and scalability. Adopting designs from chemical looping combustion, such as circulating fluidized beds or moving bed reactors, may enhance system performance. Moreover, integrating external fields (such as electric or light-driven reactors) has the potential to boost material reactivity and overall energy efficiency, although these technologies are still in the experimental stage.

System Integration and Optimization: Beyond material and reactor challenges, the integration of CLAS into industrial systems requires addressing thermal integration, system-level heat management, and cost optimization. A lack of system-wide optimization strategies,

Table 9
External assistance to reactors/systems of CLAS.

Type	Method	Detail	Example				Ref.
			Origin	Modification	Ammonia production rate (μmol $g^{-1}h^{-1}$)		
					Origin	Modification	
External field-assisted	Electro-driven	Accelerate mass transfer and reaction rates, reduce the required reaction conditions.	Thermal-driven Li_2NH	Electro-driven Li_2NH	7	64	[88]
	Light-driven		Thermal-driven Mg_3N_2	Light-driven Mg_3N_2	0	1.67	[80]
	Plasma-driven		Thermal-driven $NaNH_2$	Plasma-driven $NaNH_2$	0	550	[89]

Table 10
Comparison of different CLAS routes and the Haber-Bosch process for ammonia synthesis.

Method	Representative Materials	Conditions	Advantages	Limitations
Haber-Bosch (HB)	Fe-based catalyst, Ru-based catalyst	Temperature: 300 ~ 450℃ Pressure: 15 ~ 25 MPa	• Industrially proven and scalable • Reliable and high yield • Mature technology	• High energy consumption • High CO_2 emissions • High capital cost
H_2-MN CLAS	Mn_3N_2/Mn, Co_3Mo_3N/Co_6Mo_6N, Ca_3N_2/CaH_2	Temperature: 500 ~ 800℃ Pressure: 0.1 MPa	• Mild conditions • Metal nitrides are effective for N_2 activation Easier scale-up and safe operation	• Low NH_3 synthesis rates • Sluggish kinetics • Issues with parasitic dinitrogen formation and stability
H_2O-MN CLAS	AlN/Al_2O_3, Mo_2N/MoO_2, CrN/Cr_2O_3/Cr	Temperature: >1000℃ Pressure: 0.1 MPa	• Utilizes widely available resources • Avoids the need for high-energy hydrogen generation • Mature system design	• Requires very high temperature • Low NH_3 synthesis rates • Carbon deposition and reactor degradation
H_2-AMNH CLAS	BaNH/BaH_2, Li_2NH/LiH	Temperature: <500℃Pressure: 0.1 MPa	• High NH_3 synthesis rates • Fast kinetics • Synergy with alkali/alkaline earth metal hydrides for N_2 activation	• Inferior thermal and chemical stability • More complex operation • Deactivation due to oxidation with impurities (*e.g.*, H_2O, O_2)
Field-Assisted CLAS	Li_3N/Li+/Li, TiN, MgO, NaH	Temperature: 100 ~ 400℃ (Depends on the field)	• Potential for high energy efficiency • Overcomes thermodynamic limits via external fields (electric, plasma, light-driven) • High product selectivity and energy efficiency	• Still in small scale experimental stages • Requires complex reactor designs • Uncertain scalability and operational complexity

including thermal management and energy recycling, currently limits the potential efficiency of CLAS. Future designs must focus on optimizing process flows and integrating renewable energy sources to make CLAS a competitive alternative for ammonia production on a global scale. A schematic diagram outlining the proposed CLAS system configuration using separate solid oxide electrolysis of steam and air, along with renewable energy sources, is depicted in Fig. 10. The associated cost estimation for ammonia production via this process is also provided.

6. Conclusions and future perspectives

The synthesis of ammonia is energy-intensive, consuming 1–2 % of global energy and contributing to 1 % of carbon emissions [8]. As the demand for more sustainable production methods grows, chemical looping ammonia synthesis (CLAS) offers a promising alternative to the Haber-Bosch process. By decoupling nitrogen fixation and ammonia production, CLAS allows for optimization of the thermodynamic and kinetic properties of each step, allowing for ammonia production at or near atmospheric pressure. However, challenges such as low production rates and nitrogen carrier stability must be addressed. Future research should focus first on material selection and innovation. Transition metal nitrides (MNs) and alkali/alkaline earth metal imides (AMNHs) are currently the most promising nitrogen carriers, but their long-term stability and performance still require significant improvement. Modifying these carriers through techniques such as the introduction of dopants, promoters, or catalysts can help overcome thermodynamic and kinetic limitations. Additionally, structural modifications that increase the surface area of nitrogen carriers can enhance their reaction efficiency, making the materials more viable for large-scale operations.

As material designs evolve, it will be essential to further optimize these nitrogen carriers to improve their recyclability and stability under industrial conditions. Future studies should prioritize the development of composite systems or hybrid materials that can sustain long-term cycling without significant degradation. Moreover, a deeper understanding of reaction mechanisms through *in-situ* characterization techniques will be vital for identifying the active sites and pathways for rapid reaction and improved ammonia yield.

The design and optimization of reactors is another crucial area for future research. While current CLAS experiments rely primarily on fixed-bed reactors, transitioning to more advanced designs, such as fluidized bed reactors or moving bed reactors, will improve reaction efficiency and scalability. These reactor configurations, already proven in other chemical looping processes, could enhance the continuous operation of CLAS, enabling higher throughput and energy efficiency in industrial applications. Beyond reactor design, external field-assisted technologies represent a novel opportunity for improving both material performance and system energy efficiency. Electric and light-driven external fields have the potential to enhance nitrogen fixation and ammonia production by breaking thermodynamic equilibrium limitations, and integrating these fields into reactor systems could substantially boost overall process efficiency. While these technologies are still in the experimental phase, their development could play a pivotal role in realizing the full potential of CLAS.

However, despite these advancements, the economic feasibility of CLAS remains a key challenge when compared to the established Haber-

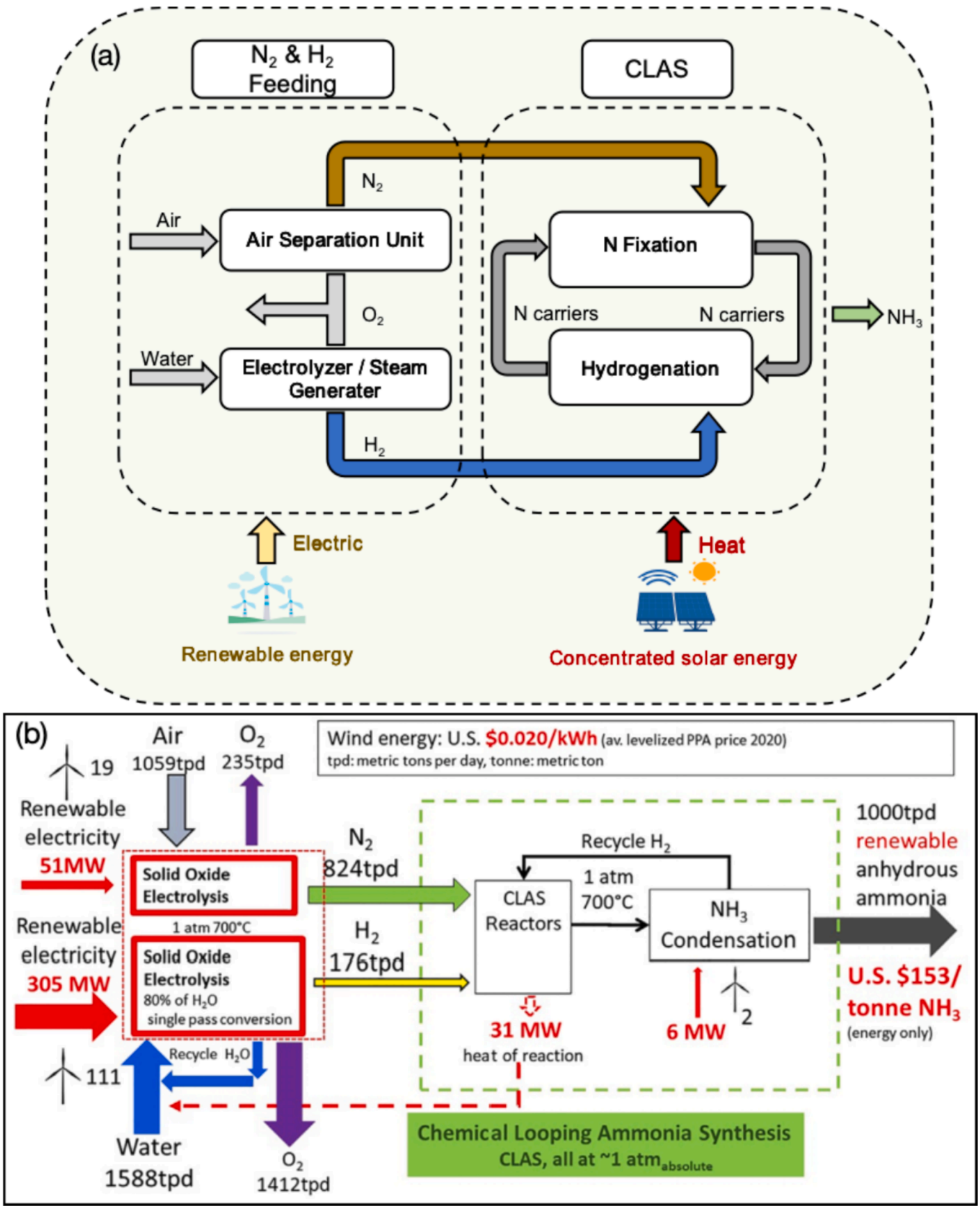


Fig. 10. Schematic of the proposed CLAS system using separate solid oxide electrolysis of steam and air with renewable energy (a), along with cost estimates for ammonia production and cost (b) [147]. Copyright 2022 AIP Publishing.

Table 11
Comparative energy costs and technical parameters for ammonia production routes (air as the N_2 resource) [12,33,147–150].

Route	Hydrogen Source	Energy Source	Process Type	Energy Cost (£/t NH_3)	Energy consumption (GJ/t NH_3)	CO_2 Emissions (t CO_2/t NH_3)	Efficiency (GJ/t NH_3)
Conventional H-B (Coke, Coal)	Coke, Coal, Heavy Fuel Oil,	Fossil Fuels (Coal, Oil)	Gasification	£205	56 ~ 64	5.32–6.18	65 %
Conventional H-B (Natural Gas)	Natural Gas, Water	Fossil Fuels (Natural Gas)	Steam Reforming	£160	28 ~ 37	1.6 ~ 1.8	70 %
Liquid H_2O Electrolysis / Air Separation / H-B	Water	Renewable (Electricity)	Liquid H_2O Electrolysis	£158	27 ~ 36	~0.5	54 %
Steam Solid Oxide Electrolysis / Air Separation /H-B	Water	Renewable (Electricity)	Solid Oxide Electrolysis	£126	20 ~ 27	~0.5	61 %
CLAS	Water	Renewable (Electricity)	Chemical Looping Process	£122	15 ~ 22	~0.1	70 %

Bosch process. While CLAS offers significant potential for reducing energy consumption and integrating renewable energy sources, scaling this technology to industrial levels presents challenges in terms of cost and long-term sustainability. The capital investment required for the development and refinement of high-performance nitrogen carriers, as well as the infrastructure needed to support CLAS, is substantial. Additionally, the intermittent nature of renewable energy sources like wind and solar may affect the continuous operation of CLAS systems, potentially leading to higher costs and reduced reliability.

Moreover, the traditional Haber-Bosch process has been optimized over the past century, making it a cost-effective and scalable solution, especially in regions with access to cheap natural gas. In contrast, CLAS technology is still in its early stages, and a comprehensive economic analysis is needed to assess its cost-effectiveness over the long term, particularly in terms of raw material availability, system design, and renewable energy integration. Table 11 illustrates the energy cost comparison between the traditional Haber-Bosch process and emerging H-B technologies, along with predictions for CLAS.

Finally, for CLAS to be truly competitive on a global scale, system-level design and optimization must be addressed. The integration of CLAS into industrial systems will require solutions for thermal management, energy recycling, and cost efficiency. Efficient heat integration and large-scale system design will be critical for improving the economic viability of CLAS.

While CLAS offers a promising path toward more sustainable ammonia synthesis, significant challenges remain in material selection, reactor design, and system integration. Addressing these challenges through continued research and technological development will be essential for the large-scale, industrial implementation of CLAS, helping to reduce global energy consumption and carbon emissions in ammonia production.

CRediT authorship contribution statement

Hangzuo Guo: Writing – original draft, Visualization, Methodology, Data curation. **Alexander R.P. Harrison:** Writing – review & editing. **Mingchen Gao:** Writing – review & editing, Data curation. **Xusheng Zhang:** Writing – review & editing, Visualization. **Qicheng Chen:** Writing – review & editing. **Zhanfeng Cui:** Writing – review & editing, Supervision, Investigation. **Binjian Nie:** Writing – review & editing, Supervision, Resources, Project administration, Investigation, Funding acquisition, Conceptualization.

Declaration of competing interest

The authors declare that they have no known competing financial interests or personal relationships that could have appeared to influence the work reported in this paper.

Acknowledgements

The work is supported by the University of Oxford Challenge Research Fund (UCSF490) and the EPSRC New Investigator Award (EP/Y015924/1).

Data availability

No data was used for the research described in the article.

References

[1] J.O. Bockris, Will lack of energy lead to the demise of high-technology countries in this century? Int. J. Hydrogen Energy 32 (2) (2007) 153–158.
[2] E.S. Van Rheenen, et al., Hydrogen carriers for zero-emission ship propulsion using PEM fuel cells: an evaluation, J. Mar. Eng. Technol. 23 (3) (2024) 166–183.
[3] J.P. Guo, P. Chen, Catalyst: NH_3 as an energy carrier, Chem 3 (5) (2017) 709–712.
[4] K. de Kleijne, et al., Worldwide greenhouse gas emissions of green hydrogen production and transport, Nat. Energy (2024).
[5] A. Salehabadi, J. Zanganeh, B. Moghtaderi, Mixed metal oxides in catalytic ammonia cracking process for green hydrogen production: A review, Int. J. Hydrogen Energy 63 (2024) 828–843.
[6] D.P. Ye, S.C.E. Tsang, Prospects and challenges of green ammonia synthesis, Nat. Synth. 2 (7) (2023) 612–623.
[7] J.W. Erisman, et al., How a century of ammonia synthesis changed the world, Nat. Geosci. 1 (10) (2008) 636–639.
[8] L. Wang, et al., Greening Ammonia toward the Solar Ammonia Refinery, Joule 2 (6) (2018) 1055–1074.
[9] M. Ravi, J.W. Makepeace, Facilitating green ammonia manufacture under milder conditions: what do heterogeneous catalyst formulations have to offer? Chem. Sci. 13 (4) (2022) 890–908.
[10] S.L. Foster, et al., Catalysts for nitrogen reduction to ammonia, Nat. Catal. 1 (7) (2018) 490–500.
[11] F. Rosowski, et al., Ruthenium catalysts for ammonia synthesis at high pressures: Preparation, characterization, and power-law kinetics, Appl. Catal. A-General 151 (2) (1997) 443–460.
[12] P.H. Pfromm, Towards sustainable agriculture: fossil-free ammonia, J. Renew. Sustain. Energy 9 (3) (2017).
[13] G. Ertl, Reactions at surfaces: From atoms to complexity (Nobel lecture), Angewandte Chemie-International Edition 47 (19) (2008) 3524–3535.
[14] T.-N. Ye, et al., Vacancy-enabled N_2 activation for ammonia synthesis on an Ni-loaded catalyst, Nature 583 (7816) (2020) 391–395.
[15] Y.X. Zhao, et al., Ammonia detection methods in photocatalytic and electrocatalytic experiments: how to improve the reliability of NH_3 production rates? Adv. Sci. 6 (8) (2019).
[16] L. Ouyang, et al., Recent advances in electrocatalytic ammonia synthesis, Chin. J. Catal. 50 (2023) 6–44.
[17] L. Hu, Z. Xing, X.F. Feng, Understanding the electrocatalytic interface for ambient ammonia synthesis, ACS Energy Lett. 5 (2) (2020) p. 430-+.
[18] G.Y. Duan, et al., Advances in electrocatalytic ammonia synthesis under mild conditions, Prog. Energy Combust. Sci. 81 (2020).
[19] H.M. Liu, et al., Homogeneous, heterogeneous, and biological catalysts for electrochemical N [reduction toward NH3 under ambient conditions, ACS Catal. 9 (6) (2019) 5245–5267.
[20] Y.H. Shi, et al., Engineering photocatalytic ammonia synthesis, Chem. Soc. Rev. 52 (20) (2023) 6938–6956.
[21] P.W. Huang, M.C. Hatzell, Prospects and good experimental practices for photocatalytic ammonia synthesis, Nat. Commun. 13 (1) (2022).
[22] R.G. Li, Photocatalytic nitrogen fixation: An attractive approach for artificial photocatalysis, Chin. J. Catal. 39 (7) (2018) 1180–1188.
[23] P. Mehta, et al., Overcoming ammonia synthesis scaling relations with plasma-enabled catalysis, Nat. Catal. 1 (4) (2018) 269–275.

[24] V.S. Gharahshiran, Y. Zheng, Sustainable ammonia synthesis: An in-depth review of non-thermal plasma technologies, Journal of Energy Chemistry 96 (2024) 1–38.
[25] D.J. Zhou, et al., Sustainable ammonia production by non-thermal plasmas: Status, mechanisms, and opportunities, Chem. Eng. J. 421 (2021).
[26] X.H. Zhang, et al., Towards green and efficient chemical looping ammonia synthesis: design principles and advanced redox catalysts, Energ. Environ. Sci. 17 (7) (2024) 2381–2405.
[27] E.K. Fu, et al., Chemical Looping Technology in Mild-Condition Ammonia Production: A Comprehensive Review and Analysis, Small 20 (1) (2024).
[28] W. Gao, et al., Thermodynamic and kinetic considerations of nitrogen carriers for chemical looping ammonia synthesis, Discover Chem. Eng. 3 (1) (2023) 1.
[29] Q.R. Wang, J.P. Guo, P. Chen, Recent progress towards mild-condition ammonia synthesis, J. Energy Chem. 36 (2019) 25–36.
[30] W.B. Gao, et al., Production of ammonia via a chemical looping process based on metal imides as nitrogen carriers, Nat. Energy 3 (12) (2018) 1067–1075.
[31] F.B. Juangsa, A.R. Irhamna, M. Aziz, Production of ammonia as potential hydrogen carrier: Review on thermochemical and electrochemical processes, Int. J. Hydrogen Energy 46 (27) (2021) 14455–14477.
[32] Q.H. Lai, et al., Chemical looping based ammonia production-A promising pathway for production of the noncarbon fuel, Sci. Bull. 67 (20) (2022) 2124–2138.
[33] H.Z. Liu, Ammonia synthesis catalyst 100 years: Practice, enlightenment and challenge, Chin. J. Catal. 35 (10) (2014) 1619–1640.
[34] T.N. Ye, et al., Contribution of nitrogen vacancies to ammonia synthesis over metal nitride catalysts, J. Am. Chem. Soc. 142 (33) (2020) 14374–14383.
[35] F. Chang, et al., Alkali and alkaline earth hydrides-driven N_2 activation and transformation over Mn nitride catalyst, J. Am. Chem. Soc. 140 (44) (2018) 14799–14806.
[36] Q. Luo, et al., A review on the synthesis of transition metal nitride nanostructures and their energy related applications, Green Energy Environ. 8 (2) (2023) 406–437.
[37] R.J.L. Pereira, I.S. Metcalfe, W.T. Hu, High-throughput screening of suitable nitrogen carriers for chemical looping ammonia synthesis, Appl. Energy Combust. Sci. 16 (2023).
[38] M.E. Gálvez, et al., Ammonia production via a two-step Al_2O_3/AlN thermochemical cycle. 2. Kinetic analysis, Ind. Eng. Chem. Res. 46 (7) (2007) 2047–2053.
[39] M.E. Gálvez, M. Halmann, A. Steinfeld, Ammonia production via a two-step Al_2O_3/AlN thermochemical cycle. 1. thermodynamic, environmental, and economic analyses, Ind. Eng. Chem. Res. 46 (7) (2007) 2042–2046.
[40] M.E. Gálvez, et al., Ammonia production via a two-step Al_2O_3/AlN thermochemical cycle. 3. influence of the carbon reducing agent and cyclability, Ind. Eng. Chem. Res. 47 (7) (2008) 2231–2237.
[41] Z.Y. Liu, et al., Selecting nitrogen carriers used for chemical looping ammonia generation of biomass and H_2O by thermodynamic method, Int. J. Hydrogen Energy 48 (10) (2023) 4035–4051.
[42] B.Y. Wang, et al., N-sorption capability of Al_2O_3-supported Mn-/Fe-based nitrogen carriers during chemical looping ammonia synthesis technology, Energy Fuel 34 (8) (2020) 10247–10255.
[43] X.Y. Wang, M.Z. Su, H.B. Zhao, Process design and exergy cost analysis of a chemical looping ammonia generation system using AlN/Al_2O_3 as a nitrogen carrier, Energy 230 (2021).
[44] Y. Wu, et al., Fe_2O_3, a cost effective and environmentally friendly catalyst for the generation of NH_3 - a future fuel - using a new Al_2O_3-looping based technology, Chem. Commun. 53 (77) (2017) 10664–10667.
[45] A. Lyngfelt, Chemical-looping combustion of solid fuels - Status of development, Appl. Energy 113 (2014) 1869–1873.
[46] Z. Liu, et al., α-Al2O3-loaded promoted the N-desorption reaction and inhibited NH3 decomposition in chemical looping ammonia generation: Experiments and DFT simulations, Int. J. Hydrogen Energy 78 (2024) 481–491.
[47] Y. Wu, et al., Promising zirconia-mixed Al-based nitrogen carriers for chemical looping of NH_3: Reduced NH_3 decomposition and improved NH_3 yield, Fuel 264 (2020).
[48] Z.Y. Liu, et al., Adsorption mechanisms of NH_3 on ZrO_2 in the N-desorption reaction of the chemical looping ammonia generation, Appl. Energy Combust. Sci. 14 (2023).
[49] Q.L. Wang, et al., A DFT study on adsorption behaviors of NH_3 and SO_2 on MnCe/TiNTs catalyst, Chem. Phys. Impact 5 (2022).
[50] M.M. Sarafraz, et al., Thermodynamic potential of a novel plasma-assisted sustainable process for co-production of ammonia and hydrogen with liquid metals, Energ. Conver. Manage. 210 (2020).
[51] Z.X. Lin, S.R. Denny, J.G. Chen, Transition metal carbides and nitrides as catalysts for thermochemical reactions, J. Catal. 404 (2021) 929–942.
[52] R. Michalsky, P.H. Pfromm, An ionicity rationale to design solid phase metal nitride reactants for solar ammonia production, J. Phys. Chem. C 116 (44) (2012) 23243–23251.
[53] R. Michalsky, P.H. Pfromm, A. Steinfeld, Rational design of metal nitride redox materials for solar-driven ammonia synthesis, Interface Focus 5 (3) (2015).
[54] R. Michalsky, et al., Chemical looping of metal nitride catalysts: low-pressure ammonia synthesis for energy storage, Chem. Sci. 6 (7) (2015) 3965–3974.
[55] A.M. Alexander, J.S.J. Hargreaves, C. Mitchell, The denitridation of nitrides of iron, cobalt and rhenium under hydrogen, Top. Catal. 56 (18–20) (2013) 1963–1969.
[56] A.M. Alexander, J.S.J. Hargreaves, C. Mitchell, The reduction of various nitrides under hydrogen: Ni_3N, Cu_3N, Zn_3N_2 and Ta_3N_5, Top. Catal. 55 (14–15) (2012) 1046–1053.
[57] S. Laassiri, et al., The potential of manganese nitride based materials as nitrogen transfer reagents for nitrogen chemical looping, Appl. Catal. B-Environm. 223 (2018) 60–66.
[58] S. Yang, et al., Molybdenum-based nitrogen carrier for ammonia production via a chemical looping route, Appl. Catal. B Environ. 312 (2022).
[59] J.S.J. Hargreaves, D. McKay, A comparison of the reactivity of lattice nitrogen in Co_3Mo_3N and Ni_3Mo_3N catalysts, J. Mol. Catal. A-Chem. 305 (1–2) (2009) 125–129.
[60] R. Michalsky, P.H. Pfromm, Chromium as reactant for solar thermochemical synthesis of ammonia from steam, nitrogen, and biomass at atmospheric pressure, Sol. Energy 85 (11) (2011) 2642–2654.
[61] W.M. Aframehr, P.H. Pfromm, Activating dinitrogen for chemical looping ammonia Synthesis: Mn nitride layer growth modeling, Chem. Eng. Sci. 252 (2022).
[62] M.G. Heidlage, et al., Thermochemical synthesis of ammonia and syngas from natural gas at atmospheric pressure, Ind. Eng. Chem. Res. 56 (47) (2017) 14014–14024.
[63] C.W. Bale, et al., FactSage thermochemical software and databases, 2010–2016, Calphad 54 (2016) 35–53.
[64] L. Burrows, P.X. Gao, G.M. Bollas, Thermodynamic feasibility analysis of distributed chemical looping ammonia synthesis, Chem. Eng. J. 426 (2021).
[65] B. Jin, et al., Thermal management for chemical looping systems with chemical production, Chem. Eng. Sci. 214 (2020).
[66] S.J. Wang, et al., Transition metal enhanced chromium nitride as composite nitrogen carrier for sustainable chemical looping ammonia synthesis, Appl. Catal. B-Environ. 339 (2023).
[67] H. Iriawan, et al., Methods for nitrogen activation by reduction and oxidation, Nat. Rev. Methods Primers 1 (1) (2021).
[68] A.J. Medford, et al., From the Sabatier principle to a predictive theory of transition-metal heterogeneous catalysis, J. Catal. 328 (2015) 36–42.
[69] D. Mckay, et al., Towards nitrogen transfer catalysis: reactive lattice nitrogen in cobalt molybdenum nitride, Chem. Commun. 29 (2007) 3051–3053.
[70] S. Al Sobhi, et al., The reactivity of lattice nitrogen within the Ni_2Mo_3N and $NiCoMo_3N$ phases, Mater. Res. Bull. 118 (2019).
[71] N. Bion, et al., The role of preparation route upon the ambient pressure ammonia synthesis activity of Ni_2Mo_3N, Appl. Catal. A-General 504 (2015) 44–50.
[72] J.L. Hua, et al., Feasibility of Fe-based nitrogen carrier for chemical looping ammonia synthesis: thermodynamics, J. Therm. Anal. Calorim. 146 (2) (2021) 673–680.
[73] A. Jafari, A. Ebadi, S. Sahebdelfar, Effect of iron oxide precursor on the properties and ammonia synthesis activity of fused iron catalysts, React. Kinet. Mech. Catal. 126 (1) (2019) 307–325.
[74] H. Fan, et al., In-Situ formation of Fe nanoparticles from FeOOH nanosheets on γ-Al_2O_3 as efficient catalysts for ammonia synthesis, ACS Sustain. Chem. Eng. 5 (11) (2017) 10900–10909.
[75] M. Hattori, et al., Enhanced catalytic ammonia synthesis with transformed BaO, ACS Catal. 8 (12) (2018) 10977–10984.
[76] R. Javaid, H. Matsumoto, T. Nanba, Influence of reaction conditions and promoting role of ammonia produced at higher temperature conditions in its synthesis process over Cs-Ru/MgO catalyst, ChemistrySelect 4 (7) (2019) 2218–2224.
[77] C.H. Xiong, et al., High thermal stability Si-Al based N-carrier for efficient and stable chemical looping ammonia generation, Appl. Energy 323 (2022).
[78] Z. Sun, et al., Ammonia synthesis via chromium-based nitrogen carrier looping, Chem. Eng. J. 476 (2023).
[79] K. Kim, et al., Electrochemical synthesis of ammonia from water and nitrogen: a lithium-mediated approach using lithium-ion conducting glass ceramics, ChemSusChem 11 (1) (2018) 120–124.
[80] D.F. Swearer, et al., Light-driven chemical looping for ammonia synthesis, ACS Energy Lett. 4 (7) (2019) 1505–1512.
[81] Z.T. Xiong, et al., Investigations into the interaction between hydrogen and calcium nitride, J. Mater. Chem. 13 (7) (2003) 1676–1680.
[82] S. Laassiri, et al., Nitrogen transfer properties in tantalum nitride based material, Catal. Today 286 (2017) 147–155.
[83] Y. Goto, A. Daisley, J.S.J. Hargreaves, Towards anti-perovskite nitrides as potential nitrogen storage materials for chemical looping ammonia production: reduction of Co_3ZnN, Ni_3ZnN, Co_3nN and Ni_3InN under hydrogen, Catal. Today 364 (2021) 196–201.
[84] S. Brown, et al., Ambient carbon-neutral ammonia generation via a cyclic microwave plasma process, ACS Appl. Mater. Interfaces 15 (19) (2023) 23255–23264.
[85] S. Yamaguchi, et al., Nitrogen dissociation via reaction with lithium alloys, ACS Omega 2 (3) (2017) 1081–1088.
[86] H.X. Yan, et al., Lithium palladium hydride promotes chemical looping ammonia synthesis mediated by lithium imide and hydride, J. Phys. Chem. C 125 (12) (2021) 6716–6722.
[87] R.Z. Wang, et al., Zn promotes chemical looping ammonia synthesis mediated by LiH-Li_2NH couple, ChemSusChem 16 (22) (2023).
[88] S. Feng, et al., Electrodriven chemical looping ammonia synthesis mediated by lithium imide, ACS Energy Lett. (2023) 1567–1574.
[89] H. Wu, et al., Plasma-driven nitrogen fixation on sodium hydride, Adv. Energy Mater. 13 (27) (2023).

[90] P.K. Wang, et al., Breaking scaling relations to achieve low-temperature ammonia synthesis through LiH-mediated nitrogen transfer and hydrogenation, Nat. Chem. 9 (1) (2017) 64–70.
[91] P.K. Wang, et al., The Formation of Surface Lithium-Iron Ternary Hydride and its Function on Catalytic Ammonia Synthesis at Low Temperatures, Angewandte Chemie-International Edition 56 (30) (2017) 8716–8720.
[92] S. Feng, et al., A multi-functional composite nitrogen carrier for ammonia production via a chemical looping route, J. Mater. Chem. A 9 (2) (2021) 1039–1047.
[93] Q.R. Wang, J.P. Guo, P. Chen, The impact of alkali and alkaline earth metals on green ammonia synthesis, Chem 7 (12) (2021) 3203–3220.
[94] B. Swain, Recovery and recycling of lithium: a review, Sep. Purif. Technol. 172 (2017) 388–403.
[95] J.M. McEnaney, et al., Ammonia synthesis from N_2 and H_2O using a lithium cycling electrification strategy at atmospheric pressure, Energ. Environ. Sci. 10 (7) (2017) 1621–1630.
[96] F.-Z. Teng, Magnesium, in: W.M. White (Ed.), Encyclopedia of Geochemistry: A Comprehensive Reference Source on the Chemistry of the Earth, Springer International Publishing, Cham, 2018, pp. 853–856.
[97] N. Ghasem, Chapter nine - Production of ammonia via chemical looping process based on metal imides as nitrogen carriers, in Progresses in Ammonia: Science, Technology and Membranes, A. Basile and M.R. Rahimpour, Editors. 2024, Elsevier. p. 205–219.
[98] T. Yamaguchi, et al., Pseudo catalytic ammonia synthesis by lithium-tin alloy, Int. J. Hydrogen Energy 45 (11) (2020) 6806–6812.
[99] K. Shinzato, et al., Systematic study on nitrogen dissociation and ammonia synthesis by lithium and group 14 element alloys, ACS Appl. Energy Mater. 5 (4) (2022) 4765–4773.
[100] A. Jain, et al., A new synthesis route of ammonia production through hydrolysis of metal-Nitrides, Int. J. Hydrogen Energy 42 (39) (2017) 24897–24903.
[101] Z.J. Tang, et al., Lithium-based loop for ambient-pressure ammonia synthesis in a liquid alloy-salt catalytic system, Chemsuschem 14 (21) (2021) 4697–4707.
[102] P. Chen, et al., Interaction of hydrogen with metal nitrides and imides, Nature 420 (6913) (2002) 302–304.
[103] J.W. Makepeace, et al., Compositional flexibility in Li–N–H materials: implications for ammonia catalysis and hydrogen storage, PCCP 23 (28) (2021) 15091–15100.
[104] W.B. Gao, J.P. Guo, P. Chen, Hydrides, amides and imides mediated ammonia synthesis and decomposition, Chin. J. Chem. 37 (5) (2019) 442–451.
[105] J.P. Guo, P. Chen, Interplay of alkali, transition metals, nitrogen, and hydrogen in ammonia synthesis and decomposition reactions, Acc. Chem. Res. 54 (10) (2021) 2434–2444.
[106] M. Ravi, J.W. Makepeace, Lithium-nitrogen-hydrogen systems for ammonia synthesis: exploring a more efficient pathway using lithium nitride-hydride, Chem. Commun. 58 (41) (2022) 6076–6079.
[107] L.H. Jepsen, et al., Thermal decomposition of sodium amide, $NaNH_2$, and sodium amide hydroxide composites, $NaNH_2$ - NaOH, PCCP 18 (36) (2016) 25257–25264.
[108] S. Hino, et al., Hydrogen desorption properties of the Ca-N-H system, J. Alloy. Compd. 398 (1–2) (2005) 62–66.
[109] Y. Nakamori, G. Kitahara, S. Orimo, Synthesis and dehydriding studies of Mg-N-H systems, J. Power Sources 138 (1–2) (2004) 309–312.
[110] W.B. Gao, et al., Barium hydride activates Ni for ammonia synthesis catalysis, Faraday Discuss. 243 (2023) 27–37.
[111] Y.Q. Guan, et al., Transition-Metal-Free Barium Hydride Mediates Dinitrogen Fixation and Ammonia Synthesis, Angewandte Chemie-International Edition 61 (39) (2022).
[112] W.B. Gao, et al., Barium hydride-mediated nitrogen transfer and hydrogenation for ammonia synthesis: a case study of cobalt, ACS Catal. 7 (5) (2017) 3654–3661.
[113] K. Tagawa, et al., Improvement of kinetics of ammonia synthesis at ambient pressure by the chemical looping process of lithium hydride, J. Phys. Chem. C 126 (5) (2022) 2403–2409.
[114] Y.H. Hu, E. Ruckenstein, Ultrafast reaction between Li_3N and $LiNH_2$ to prepare the effective hydrogen storage material Li_2NH, Ind. Eng. Chem. Res. 45 (14) (2006) 4993–4998.
[115] R.J.L. Pereira, W. Hu, I.S. Metcalfe, Impact of gas-solid reaction thermodynamics on the performance of a chemical looping ammonia synthesis process, Energy Fuel 36 (17) (2022) 9757–9767.
[116] Q. Wei, et al., Ammonia separation from N_2 and H_2 over LTA zeolitic imidazolate framework membranes, J. Membr. Sci. 623 (2021) 119078.
[117] M. Malmali, et al., Better Absorbents for Ammonia Separation, ACS Sustain. Chem. Eng. 6 (5) (2018) 6536–6546.
[118] A. Tosello Gardini, U. Raucci, M. Parrinello, A bulk phase transformation drives ammonia synthesis on barium hydride, Chemrxiv (2024).
[119] G.A. Somorjai, N. Materer, Surface structures in ammonia synthesis, Top. Catal. 1 (3–4) (1994) 215–231.
[120] G. Selvaduray, L. Sheet, Aluminum nitride - review of synthesis methods, Mater. Sci. Technol. 9 (6) (1993) 463–473.
[121] R. Michalsky, P.H. Pfromm, Thermodynamics of metal reactants for ammonia synthesis from steam, nitrogen and biomass at atmospheric pressure, AIChE J 58 (10) (2012) 3203–3213.
[122] Q. Wang, et al., Carbothermal synthesis of spherical AlN granules: Effects of synthesis parameters and Y_2O_3 additive, Ceram. Int. 41 (5) (2015) 6715–6721.
[123] Q. Zhang, et al., High-performance mesoporous (AlN/Al_2O_3) for enhanced NH_3 yield during chemical looping ammonia generation technology, Int. J. Hydrogen Energy 45 (16) (2020) 9903–9913.
[124] A.L. Molisani, H.N. Yoshimura, Low-temperature synthesis of AlN powder with multicomponent additive systems by carbothermal reduction-nitridation method, Mater. Res. Bull. 45 (6) (2010) 733–738.
[125] M.K. Fu, et al., Thermodynamic analysis of novel vanadium redox materials for solar thermochemical ammonia synthesis from N_2 and CH_4, Int. J. Hydrogen Energy 45 (4) (2020) 2569–2577.
[126] D. Mckay, et al., The influence of phase and morphology of molybdenum nitrides on ammonia synthesis activity and reduction characteristics, J. Solid State Chem. 181 (2) (2008) 325–333.
[127] B.F. Cao, et al., Mixed close-packed cobalt molybdenum nitrides as non-noble metal electrocatalysts for the hydrogen evolution reaction, J. Am. Chem. Soc. 135 (51) (2013) 19186–19192.
[128] A.Y. Ganin, L. Kienle, G.V. Vajenine, Synthesis and characterisation of hexagonal molybdenum nitrides, J. Solid State Chem. 179 (8) (2006) 2339–2348.
[129] S. Bhattacharyya, et al., Synthesis and magnetic characterization of $CoMoN_2$ nanoparticles, J. Nanopart. Res. 12 (4) (2010) 1107–1116.
[130] S.A. Rasaki, et al., Synthesis and application of nano-structured metal nitrides and carbides: a review, Prog. Solid State Chem. 50 (2018) 1–15.
[131] S.Y. Yun, et al., Ammonolysis-driven exsolution of Ru nanoparticle embedded in conductive metal nitride matrix to boost electrocatalyst activity, Adv. Sci. 11 (24) (2024).
[132] J. Puig, M. Balat-Pichelin, Production of metallic nanopowders (Mg, Al) by solar carbothermal reduction of their oxides at low pressure, J. Magnes. Alloys 4 (2) (2016) 140–150.
[133] M.E. Gálvez, et al., Solar hydrogen production via a two-step thermochemical process based on MgO/Mg redox reactions - thermodynamic and kinetic analyses, Int. J. Hydrogen Energy 33 (12) (2008) 2880–2890.
[134] Q.R. Wang, et al., Thermodynamic Properties of Ammonia Production from Hydrogenation of Alkali and Alkaline Earth Metal Amides, ChemPhysChem 20 (10) (2019) 1376–1381.
[135] H.J. Cao, et al., Transition and alkali metal complex ternary amides for ammonia synthesis and decomposition, Chem. A Europ. J. 23 (41) (2017) 9766–9771.
[136] Y. Gao, et al., N-desorption or NH_3 generation of TiO_2-loaded Al-based nitrogen carrier during chemical looping ammonia generation technology, Int. J. Hydrogen Energy 43 (34) (2018) 16589–16597.
[137] N. Shan, et al., Fe and Ni dopants facilitating ammonia synthesis on Mn_4N and mechanistic insights from first-principles methods, J. Phys. Chem. C 122 (11) (2018) 6109–6116.
[138] N.N. Shan, et al., Manipulating the geometric and electronic structures of manganese nitrides for ammonia synthesis, ChemCatChem 12 (8) (2020) 2233–2244.
[139] W.M. Aframehr, P.H. Pfromm, Activating dinitrogen for chemical looping ammonia synthesis: nitridation of manganese, J. Mater. Sci. 56 (22) (2021) 12584–12595.
[140] W.M. Aframehr, C.R. Huang, P.H. Pfromm, Chemical Looping of Manganese to Synthesize Ammonia at Atmospheric Pressure: Sodium as Promoter, Chem. Eng. Technol. 43 (10) (2020) 2126–2133.
[141] S. Laassiri, et al., Combination of theoretical and experimental investigations of the role of lithium dopant in manganese nitride: a two-stage reagent for ammonia synthesis, Faraday Discuss. 229 (2021) 281–296.
[142] K. Honkala, et al., Ammonia synthesis from first-principles calculations, Science 307 (5709) (2005) 555–558.
[143] A. Mishra, F.X. Li, Chemical looping at the nanoscale - challenges and opportunities, Curr. Opin. Chem. Eng. 20 (2018) 143–150.
[144] M.L. Qin, et al., Synthesis of aluminum nitride powder by carbothermal reduction of a combustion synthesis precursor, Mater. Res. Bull. 43 (11) (2008) 2954–2960.
[145] M. Uysal, et al., The preparation of core-shell Al_2O_3/Ni composite powders by electroless plating, Ceram. Int. 39 (5) (2013) 5485–5493.
[146] D.W. Wang, Y.T. Zhang, L.S. Fan, Chemical looping process for hydrogen and electricity co-production: Design and operational consideration for moving-bed-reducer-based circulating fluidized bed systems, Powder Technol. 431 (2024).
[147] P.H. Pfromm, W. Aframehr, Green ammonia from air, water, and renewable electricity: Energy costs using natural gas reforming, solid oxide electrolysis, liquid water electrolysis, chemical looping, or a Haber-Bosch loop, J. Renew. Sustain. Energy 14 (5) (2022).
[148] D. Xiang, et al., A chemical looping scheme of co-feeding of coke-oven gas and pulverized coke toward polygeneration of olefins and ammonia, Chem. Eng. J. 334 (2018) 1754–1765.
[149] X. Niu, L.H. Shen, Evolution of carbon and nitrogen during chemical looping gasification of rapeseed cake with Ca-Fe oxygen carrier, Chem. Eng. J. 431 (2022).
[150] J.P. Tang, L.X. Kang, Y.Z. Liu, Design and optimization of a clean ammonia synthesis system based on biomass gasification coupled with a Ca-Cu chemical loop, Ind. Eng. Chem. Res. 61 (23) (2022) 8128–8140.